Contents lists available at ScienceDirect

Renewable and Sustainable Energy Reviews

journal homepage: www.elsevier.com/locate/rser

Theoretical limits of photovoltaics efficiency and possible improvements by intuitive approaches learned from photosynthesis and quantum coherence

Fahhad H. Alharbi [a,*], Sabre Kais [a,b]

[a] Qatar Energy and Environment Research Institute (QEERI), Doha, Qatar
[b] Department of Chemistry, Physics and Birck Nanotechnology Center, Purdue University, West Lafayette, IN 47907, United States

ARTICLE INFO

ABSTRACT

In this review, we present and discussed the main trends in photovoltaics (PV) with emphasize on the conversion efficiency limits. The theoretical limits of various photovoltaics device concepts are presented and analyzed using a flexible detailed balance model where more discussion emphasize is toward the losses. Also, few lessons from nature and other fields to improve the conversion efficiency in photovoltaics are presented and discussed. From photosynthesis, the perfect exciton transport in photosynthetic complexes can be utilized for PV. Also, we present some lessons learned from other fields like recombination suppression by quantum coherence. For example, the coupling in photosynthetic reaction centers is used to suppress recombination in photocells.

Contents

---

* Corresponding author.
E-mail addresses: falharbi@qf.org.qa (F.H. Alharbi), sakais@qf.org.qa (S. Kais).

1. Introduction

Sunlight is the most abundant energy source available on earth, and therefore designing systems that can effectively gather, transfer, or store solar energy has been a great enduring interest for researchers. Maybe the most apparent field in this regard is photovoltaics (PV). PV effect was known for about two centuries [1]. However, its serious technological development started in the 1950s. Various materials and device concepts have been developed since then and high conversion efficiencies have been achieved (44.7% using quadruple junction [2]). This great development in the efficiency is not matched if the cost of the device is considered. The highly efficient PVs (mainly multi-junction solar cells) are prohibitively expensive [3,4]. On the other hand, the efficiency of the most dominant technology in the market (i.e. Si) is 25% in the lab and less than 20% commercially. In a very interesting recent development, the hybrid perovskites solar cell ((CH_3NH_3)PbI_3) has attracted an extraordinary attention [5–9] as its efficiency has jumped to 17.9% in about 4 years [10]. Beyond that, the research trends have been wide spread though heavily material driven. One of the main research and development directions is to find cheaper and efficient absorbers. This is very crucial as the main limiting factor for PV deployment is the cost. Other efforts focus on developing alternative device concepts like multijunction and tandem solar cells. Another important direction is toward reducing the "fundamental" losses in the cells; but it proves to be very challenging.

Recently, new trends have appeared to utilize intuitive approaches learned from other fields like photosynthesis and lasers. In light harvesting organisms, the major mechanism that converts light energy into chemical energy is photosynthesis. Remarkably, in plants, bacteria and algae, the photon-to-charge conversion efficiency is about 100% under certain conditions [11]. This fact is of great interest and generate a lot of excitement to understand how nature optimized different molecular processes such as trapping, radiative, and non-radiative losses, and in particular the role of quantum coherence to enhance transport in photosynthesis [12–14]. This might lead to allow engineering new materials mimicking photosynthesis and could be used to achieve similar performances in artificial photosynthesis-based solar cells [15,16]. Quantum mechanics which was developed in the twentieth century continues to yield new fruit in the twenty-first century. For example, quantum coherence effects such as lasing without inversion [17,18], the photo-Carnot quantum heat engine [19], photosynthesis, and the quantum photocell [20] are topics of current research interest which are yielding new insights into thermodynamics and optics.

In this review, we present collectively, different PV device concepts and the theoretical limits for their efficiencies where more discussion emphasize is toward the losses. However, a better understanding of the losses shall provide new insights. For the analysis, a detailed balance model is used, where the balance is maintained between two-extended-level system that are affected by solar radiation and the consequences like excitation and recombination [21,22]. The model is flexible and hence can be altered to accommodate all the analyzed device concepts. Then, we described in some details photosynthesis and some quantum aspects from which lessons can be utilized in PV field.

2. Photovoltaics: alternative devices concept

The general concept of solar cell is simple. An electron should be excited by solar radiation and then it should be collected at the anode before it losses the gained energy totally. Then the electron will be reinjected with energy below Fermi level E_F into the cell from the cathode. The energy difference of the electron (between its energy at anode where it is collected and the energy at the cathode where it is reinjected) is used to do work (electrically, voltage times current). The cell should be designed so that the collection site (high-energy) cannot supply carriers to the injection site (low-energy) as this will result in wasting the energy of the excited electron. The concept is presented schematically in Fig. 1.

Conceptually, the semiconductors are not essential to realize photovoltaic effect though they are used in all solar cells now. In dye sensitized solar cells (DSSC), the semiconductors (i.e. ZnO and TiO_2) are not used because of their semiconducting properties; they are merely used as an electron carrier and hole blocker. However, using semiconductors is currently the most convenient way to prevent losing all the energy gained by the excited electron. Practically there are two possible ways to ensure gaining energy; namely by the energy gap (E_g) in the semiconductors or very fast collection as shown in Fig. 2. In the semiconductor, the excited carriers are relaxing back to the edge of the conduction and valance band.

Photovoltaics effect was known for about two centuries. In 1839, Becquerel observed the effect accidentally while working on electrolytic cells [23,24]. The first all-solid cell was made by Adams and Day in 1876 using selenium [1]. Later in the century, a set of PVs patents appeared [25–28]. More efforts were conducted in the subject afterwards; but, the efficiency remains extremely small. The practical realization was achieved in 1950, when a 6% Si solar cell was made in Bell Labs [29] and then used for space applications. At that time, the work was based heavily on the conventional semiconductors and it was mainly to prove the concept. By 1960, 14% efficient Si solar cells was made [30]; but, it was
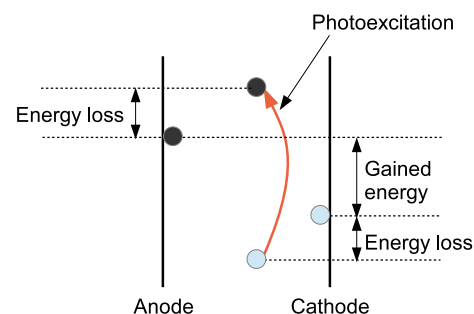
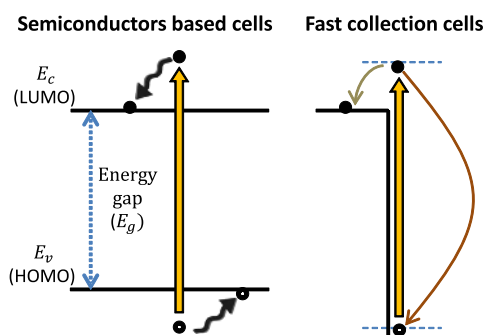**Fig. 1.** The general concept of solar cell operation.

Fig. 2. The practical means to ensure gaining energy before it is lost totally. In the left, the gap in the semiconductors prevents the excited electron returning back to its originally lower energy position. In the right, the excited electron can be collected very rapidly by injection (green curved arrow) to electron carrier layer before it recombine (brown curved arrow). (For interpretation of the references to color in this figure caption, the reader is referred to the web version of this paper.)

prohibitively expensive and not commercially lucrative. Thus, the need to reduce the cost lead to the second generation solar cells.

The work in the second generation solar cells started in the early 1960s where the aim was to reduce the fabrication cost of the solar cells in a trade of reduced efficiency. One of the most explored directions was to use alternative semiconductor absorbers. Tens of semiconductors were explored [31–36] and the most prominent solar cells of that era were those based on CdTe and Cu (In$_G$a)Se$_2$ (CIGS), which are thin film cells. Their current record efficiencies are 20.4% for CdTe [37] and 20.8% for CIGS [38]. At the same era, Si based cell has been improved remarkably and its current efficiency record is 25% which is about 8% less than the theoretical limit [21,22,39]. Some thorough theoretical analyses with more restricted practical assumptions indicated that the limit is not far above the obtained efficiency [40].

Currently, we are in the midst of the third generation solar cell stage. The main aim of this stage is to make the electricity production cost of solar cells commercially competitive by reducing the cell fabrication costs and elevating the efficiencies above Shockley and Queisser limit [32–34,36]. The developments have taken many directions, which can be categorized in different forms. In this paper, we categorize them based on the device concept as this is used later for the theoretical limits analysis. In each category, some of the active research areas are briefly presented. Research activities, that are more toward conventional materials processing, are not addressed.

2.1. Single junction devices

2.1.1. Alternative inorganic materials
Conceptually, many inorganic semiconductors have the required physical properties to make efficient solar cells [31,33,35]. However, few of them have been extensively explored [33–35]. This area was very active in the 1970s and faded in the late 1980s. With the growing interest in solar energy, it has started gaining growing attentions in the recent years [32–34,36]. The best obtained efficiencies of alternative absorbers are 17.1% and 12.0% for WSe$_2$ [41] and MoSe$_2$ [42], respectively. For both of them, the device design was electrochemical cell. For all solid cell, the best efficiency is 8.0% for WSe$_2$ absorber forming a heterojunction with ZnO [43].

2.1.2. Organic photovoltaics (OPV)
Organic semiconductors have been known for long time and they have been used in many relevant applications. For solar energy, Tang reported the first organic heterojunction solar cell in 1984 [44]. Since then, OPV field has been very active especially in

the past few years as the maximum obtained efficiency was almost doubled [45–49] between 2009 (about 6%) and now where the efficiency reached 11.1% [49].

2.1.3. Sensitized solar cells
In 1988, Gratzel reintroduced the concept of dye sensitized solar cell (DSSC) with liquid electrolyte [50–53]. It has attracted tremendous attention since then. the concept was introduced first by Gerischer [54,55] and improved by Fujihira [56,57], Weller [58,59], and others. Practically, DSSC is a monolayer solar cell as the transport between the dyes is very small and having multiple dye layers causes a lot of practical challenges. Despite this fact, the device concept is very efficient and the latest obtained efficiency is 13.4% [60]. Furthermore, enormous types of dyes have been explored. One of the most interesting developments is the availability of solid based electrolyte [59,61–63]. Also, it has been demonstrated that inorganic nanoparticles can replace the dye as sensitizer [64–68].

2.1.4. Hybrid perovskites
Recently, the hybrid perovskites solar cell ((CH$_3$NH$_3$)PbI$_3$) has attracted an extraordinary attention [5–9] as its efficiency has jumped to 17.9% in about 4 years [10]. The absorbing perovskites are a special family of hybrid organic–inorganic crystalline materials with AMX$_3$ perovskite structure, where A is the organic site, M is a metal, and X is a halogen [7,69–71]. The structure, which seems complex chemically, is extremely rich and can be grown and controlled relatively easily with high quality [8,69,70,72–74]. It has been used for many applications [75–77] and its applicability for solar cells was anticipated very early [78]. However, the real thrust to make solar cells out of them is very recent [5–9,71,72]. In this short time, an efficiency of 17.9% was reported [10] and it is expected that 20%+ efficiency can be achieved within few years [71,72].

2.1.5. Nanostructured solar cells
In the past two decades, the developments in nanotechnology have contributed a lot to introduce structures, materials, and mechanisms in solar cells that are not possible in bulk form [64,67,68,79–84]. Among the effects are energy gap E_g tunability, absorption, and transport direction decoupling, and three-dimension structuring. However, due to the size related challenges, the obtained efficiencies are still small. Practically, nanostructuring results in deteriorated transport mainly due to interracial defects [22,85–87]. The best obtained efficiency in such structures is 8.55% with PbS quantum dots [88].

2.2. Multi-cell devices

2.2.1. Multijunction solar cells
The long history and success of III–V optoelectronics allowed a smooth deployment of them in solar cell industry [89–92] especially for the challenging structures like the multijunction cells. In such systems, few layers of different E_g cells are stacked in series where in-between buffer layers allow transporting the photo-generated carriers between the layers. The system is two-terminal device as shown in Fig. 3. Its best obtained efficiency is 44.7% [2] with quadruple junction developed by Fraunhofer ISE. However, there are many technological challenges that limit it such as the essentiality of current continuity, lattice matching, and the tunnelling of photo-generated carriers. Commercial wise, it is extremely expensive to fabricate [3,4] and this fact limits it to few applications. To distinguish it from the other concepts of multi-cell devices, it is represented schematically in Fig. 3 and as shown,
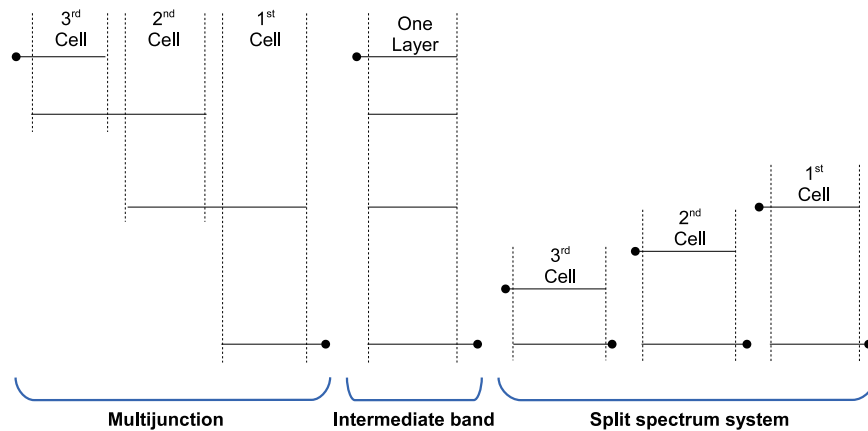
Fig. 3. The concepts of multijunction (left), intermediate band (center), and split spectrum (right) solar cell systems. The dots are the collection (injection) points.

it is conceptually a two-terminal system with a series stack of two-level cells.

2.2.2. Intermediate band cells

In such cells, the multi-photon absorption occurs in a single material layer and obviously, multi-level system is needed as represented in Fig. 3. The concept is relatively new and far from maturity as it is introduced by Luque and Marti in 1997 [79,93,94]. Although the concept is plausible, there are many challenges that should be resolved [95] and the obtained efficiencies based on this concept are small. Practically, there are two main trends to realize such system. The first one is based on doping large E_g materials to create extended defect bands in the gap [94,96,97]. The second trend depends on super-lattices and organized quantum dots where many separated states can be created due to quantum size effects [98–100].

2.2.3. Split spectrum solar cell system

The main idea of this system is to split solar radiation by a pre-optical setup and then direct each of the split spectrum into a cell with matching E_g [101–104]. So, the system is composed of two parts. The first one is the optical system that splits the spectrum and concentrates the light. The second part is the set of SCs to be used to harvest the energy from the split spectrums as shown in Fig. 3. This avoids two of the main challenges that faces multi-junction and intermediate band solar cells; namely current continuity and lattice matching in the case of multijunction cells and current continuity in intermediate band cells. The idea is not new and it has been suggested in 1955 [101] and patented in 1960 [105] by Jackson. Some initial devices were developed in the 1970s. Moon et al. demonstrated 28.5% two-cell system in 1978 [102]. The record was set by Green and Ho-Baillie who obtained 43.5% efficiency using 5-cell system [103]. Recently, it has been shown that a 50%+ efficiency could be obtained using nowadays technologies [104].

2.3. Thermalization control based devices

2.3.1. Carrier multiplication devices

As known – and to be shown, thermalization results in most losses in solar cells. The excess absorbed photon energy (above E_g) is lost as the hot carrier is relaxed into the band edge. The concept of carrier multiplication (CM) is based on utilizing the energetic photon to generate multiple electron–hole pairs before it relaxes. Experimentally, CM has been demonstrated for both bulk and quantum sized semiconductor systems. Remarkably, Schaller and Klimov group achieved seven-fold multiplication in PbSe and PbS

quantum dots (QDs) [106]. However, almost all CM experiments are done under unpractical conditions for solar cells. This fact and many other challenges have been highlighted repeatedly [22,107–109].

2.3.2. Hot carrier collection

The idea of such cell concept is to collect the excited electron hot before it relaxes completely [110,111]. In principle, this can be achieved by enabling very fast photo-current collection, using selected contacts, or slowing down the relaxation [112–114]. Recently, it has been demonstrated that some nano materials like graphene enable – expectedly – hot carrier transport [115–117].

2.4. Spectrum manipulation based devices

2.4.1. Up- and down-conversion cells

Solar radiation has a very broad spectrum ranging from far infra-red into ultraviolet (around 4 eV). So, designing a device that utilize all the possible energy is challenging. The idea of up- and down- conversion cells is to manipulate the spectrum by various optical nonlinear systems to reduce the width of the resulted spectrum and then use the proper cell for energy harvesting [118,119]. Such spectrum manipulation can extremely reduce the losses due to thermalization. However, the nonlinear conversion is a challenge by itself.

2.4.2. Thermophotovoltaics (TPV)

The idea of such device is to utilize the generated heat (by photovoltaic losses) to generate extra electricity beside the photo-voltaic output [120–124]. So, it consists basically of a thermal emitter and a photovoltaic. For the thermal emitter and to create more heat differential, it is common to use optical concentration with the system. The theoretical limit is far beyond that of the solar cells and many analyses show that the limit is just above 80% [123,125–127] (this is far beyond solar cell limits). The area is rich and many device designs and materials have been explored. However, the reported efficiencies are still small [123,125].

3. Energy conversion theoretical limits for various PV device concepts

Theoretically, many models were used to estimate the maximum possible efficiencies of the solar cells. They can be categorized in two general families. The first category analyses are phenomenologically based on detailed balance of radiations between two-extended-level system. This accounts for excitation and radiative recombination. Originally, this was introduced by

Shockley and Queisser in 1961 [39] and then followed by many others [21,22,128–131]. In this review, we use a model of this category [21,22]. It will be presented later. The second category is more fundamental and it is fully thermodynamical. These models are based on maintaining the balance of both energy and entropy fluxes [40,132,133].

Practically and as mentioned in the previous subsection, there are many possible operation concepts of solar cells. To estimate the upper limit of each device concept, different assumptions are made. Here listed are the main assumptions that are taken commonly in considerations:

- Solar radiation strength and spectrum vary based on the position and system design. For example, the spectrum on satellites is different from that on earth surface as some spectrum lines are absorbed by gases on the atmosphere. Also, the strength and the spectrum can be altered by using pre-optical systems like concentrator and spectrum manipulation. This can be calculated from the base solar radiation. In this review, we assume AM1.5G photon flux ($\phi_{1.5}$) where the reference solar spectra ASTMG -173-03 (American Society for Testing and Materials) [134,135] is used.
- Any incident photon above the energy gap E_g of the used cell is absorbed.
- Any photon (with energy E) shall produce $\gamma(E)$ electrons, where γ is the multiplication factor. In most cases, $\gamma = 1$. Yet, if carrier multiplication is possible, it can take higher values. This will be included in the analysis.
- There are many recombination mechanisms. Many of them – and unfortunately, the most effective ones – are caused by material quality, device design, and fabrications. Such non-fundamental mechanisms do not set the upper limit. The main unavoidable recombination mechanism is the one due to spontaneous emission. This is governed by the generalized black body radiation as will be shown later. In this work, this mechanism is forced as it is inevitable.

3.1. Single junction solar cells

In this review, a detailed balance model is used to estimate the upper efficiency limits under different conditions [21,22]. The balance is applied to the radiations in two-extended-level system. The first studied device structure is for single junction solar cells. As a radiation of flux $\phi(E)$ reaches the cell, the photo-generated current is then

$$J_g(E_g) = q \int_{E_g}^{\infty} \gamma(E)\phi(E) \, dE \tag{1}$$

where E_g is the energy gap (in eV), q is the electron charge, E is the photon energy (in eV), and $\gamma(E)$ is the multiplication as mentioned above. $\phi(E)$ in this case can be any manipulation of the base AM1.5G standard flux. Two cases will be considered in this work. The first one is to assume that the whole flux get to the cell without concentration and loss. The second case is with uniform optical concentration where the flux is simply multiplied by a factor X that represents the uniform concentration.

As the recombination is assumed to be only due to spontaneous emission which is governed by the generalized black body radiation, the recombination current can be calculated accordingly and it is

$$J_r(E_g, V, T) = qa \int_{E_g}^{\infty} \frac{E^2}{\exp\left(\frac{E - \gamma(E)V}{kT}\right) - 1} \, dE \tag{2}$$

where

$$a = \left(\frac{2\pi q^3}{c^2 h^3}\right), \tag{3}$$

c is the speed of light in vacuum in m/s, h is Planck's constant in eV s, V is the photo-generated voltage across the cell in V, k is Boltzmann's constant (in eV/K), and T is the temperature (in K). So, the net current is then just the remaining photo-generated current after the recombination losses. So,

$$J(E_g, V, T) = J_g(E_g) - J_r(E_g, V, T) \tag{4}$$

Then, the conversion efficiency can be calculated directly as the ratio between the output and input power

$$\eta(V) = \frac{P_{out}}{P_{in}} = \frac{VJ(E_g, V, T)}{P_{in}} \tag{5}$$

where P_{in} is the input power and it equals to

$$P_{in} = q \int_{0}^{\infty} E\phi(E) \, dE \tag{6}$$

The maximum possible efficiency at given E_g and T is obtained by varying V to maximize η.

There are three main causes of losses in this model. The first one is due to the unabsorbed photons where its loss fraction is

$$L_{unabs}^{(SJ)} = \frac{q}{P_{in}} \int_{0}^{E_g} E\phi(E) \, dE \tag{7}$$

The second cause is due to thermalization where the loss is the difference between the energy of the absorbed photon (i.e. E) and the energy gained by its photo-generated electrons (i.e. $\gamma(E)V$). So,

$$L_{th}^{(SJ)} = \frac{q}{P_{in}} \int_{E_g}^{\infty} (E - \gamma(E)E_g)\phi(E) \, dE \tag{8}$$

The last loss is to recombination and it is

$$L_r^{(SJ)} = \frac{VJ_r}{P_{in}} + \frac{q}{P_{in}} \int_{E_g}^{\infty} (E_g - V)\gamma(E)\phi(E) \, dE \tag{9}$$

The first term is the direct loss due to the recombination. The second term accounts for the further thermalization as a result of the balance between absorption and re-emission where the extracted photo-generated current gained V potential instead of separation energy after initial relaxation (i.e. E_g).

In the first analysis, η is optimized for operation at room temperature ($T = 300$ K) for different E_g's and with no carrier multiplication (i.e. $\gamma = 1$). The corresponding $L_{unabs}^{(SJ)}$, $L_{th}^{(SJ)}$, and $L_r^{(SJ)}$ are calculated as well as shown in Fig. 4. The maximum obtainable efficiency is 33.3% at $E_g = 1.14$ eV, which is very close to silicon E_g.
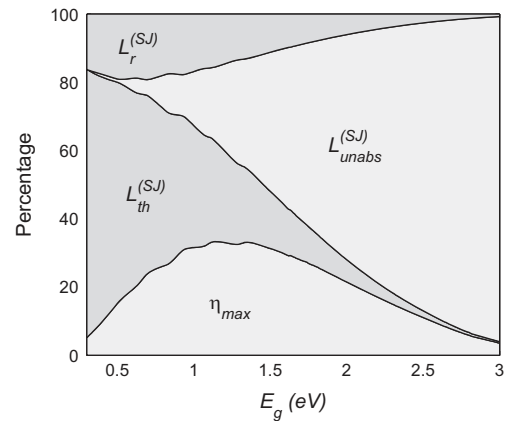

Fig. 4. The optimized η of single junction solar cells for different E_g's at $T = 300$ K and with no carrier multiplication. The corresponding $L_{unabs}^{(SJ)}$, $L_{th}^{(SJ)}$, and $L_r^{(SJ)}$ for each E_g are added up.

However, there is a wide window of energy gaps between 0.91 eV and 1.57 eV that has efficiency limit about 30%. Many semiconductors have gaps in this range and can conceptually be used to develop relatively efficient single-junction solar cells providing that the transport is good.

Over the whole range of E_g, more that 50% of energy is lost either due to thermalization or for not absorbed photons. This particular fact is the essence of many efforts to increase conversion efficiency. This is why device concepts such as multi-junction, split-spectrum, hot carrier, and carrier multiplication cells were introduced. Eqs. (7) and (8) show that these losses are – ideally – independent of temperature and the balance between absorption and re-emission (characterized by the gained potential V). Furthermore and ideally, they both are not affected by uniform optical concentration, where ϕ is simply concentrated to $X\phi$. So, all quantities depend linearly on ϕ and will be affected accordingly. From, Eqs. (6)–(8), it can be shown that both $L_{unabs}^{(SJ)}$ and $L_{th}^{(SJ)}$ remain constant with uniform optical concentration. So, before considering the other device concepts, we will consider the effects of temperature and optical concentration on single junction cell efficiency limits and mainly on η_{max} and $L_r^{(SJ)}$.

First, it can be observed from Fig. 4 that the recombination loss is quite large at small E_g and it then gets reduced. Fig. 5 shows the ratio between $L_r^{(SJ)}$ and η_{max}. At small E_g (up to about 0.59 eV), the losses due to recombination are more than the obtained conversion. Even at higher E_g, a good portion of energy conversion is lost due to the recombination.

From Eq. (9), it is clear that the main cause for $L_r^{(SJ)}$ is the recombination current J_r, in which the denominator of the integrand depends on T (Eq. (2)). To absorb the photon, E should be greater than $\gamma(E)V$. So, the integrand will increase with T and hence J_r. So, η_{max} should improve as T decreases. This is actually the case as shown in Fig. 6 as $L_r^{(SJ)}$ decreases with T (Fig. 7). At very low temperature, the maximum efficiency limit is 48.48% at 1.12 eV gap. However, the window of E_g of the highest obtainable conversion is slightly red-shifted to become between 0.86 eV and 1.40 eV for limits about 45%.

The other way to reduce relatively the effects of J_r is to concentrate the incident solar radiation. In this case, both J_g and P_{in} increase linearly with ϕ. So, by X uniform concentration, the conversion efficiency becomes

$$\eta(V) = \frac{V\left(J_g - \dfrac{J_r}{X}\right)}{P_{in}} \tag{10}$$

Fig. 8 shows how the efficiency improves with X as $L_r^{(SJ)}$ is reduced with increasing X (Fig. 9). At 500 sun concentration, η_{max} gets to 40.04% at 1.12 eV gap.

Clearly, the effect of the temperature on η_{max} is more than that of the concentration. This is further represented in Figs. 10 and 11. At very large X, the effects will coincide. Practically, optical concentration is easier to realize. However, it results in more complications as the temperature of the system increases and it commonly results in efficiency reduction and mechanical challenges. This imposes using cooling systems in the concentrated solar cells. On the other hand, operating in very low temperature is not practical. However, some device concepts may mimic that.

Fig. 6. The contour of η_{max} vs. E_g and temperature for a single junction solar cell and with no optical concentration.

Fig. 7. The contour of $L_r^{(SJ)}$ vs. E_g and temperature for a single junction solar cell and with no optical concentration.
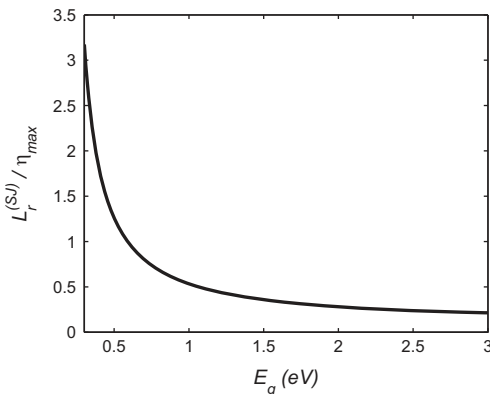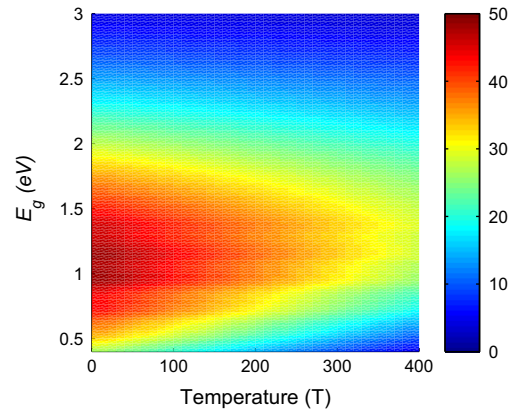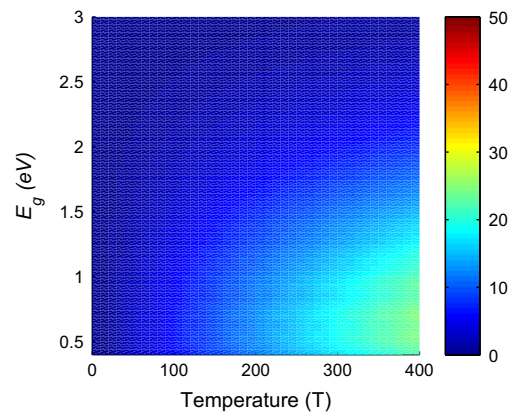
Fig. 5. The ratio between $L_r^{(SJ)}$ and η_{max} of single junction solar cells for different E_g's at $T = 300$ K and with no carrier multiplication.
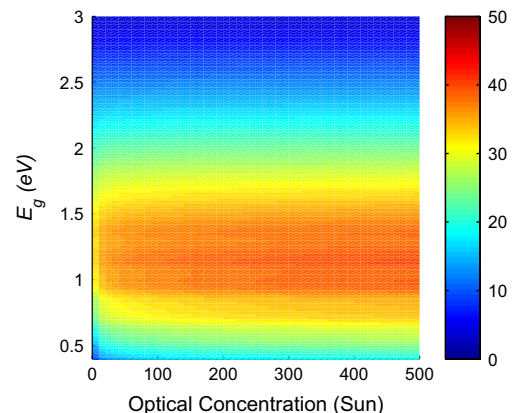
Fig. 8. The contour of η_{max} vs. E_g and X for a single junction solar cell at 300 K.
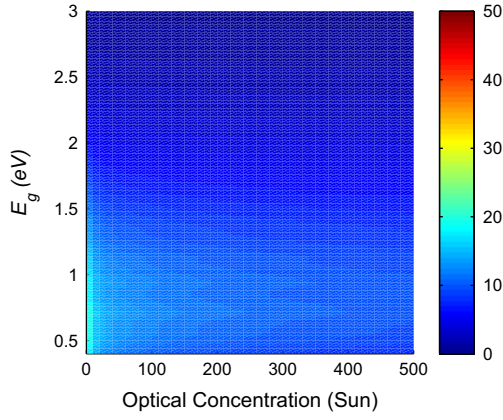
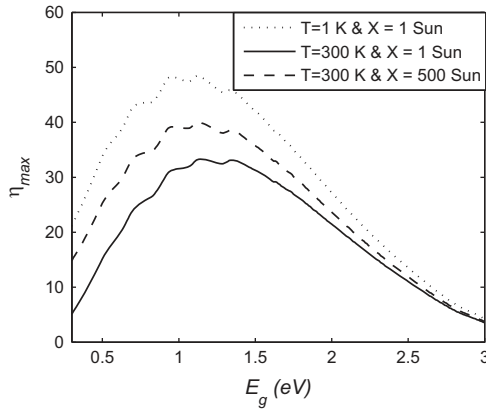Fig. 9. The contour of $L_r^{(SJ)}$ vs. E_g and X for a single junction solar cell at 300 K.

Fig. 10. η_{max} vs. E_g for a single junction solar cell at different optical concentration and temperature.
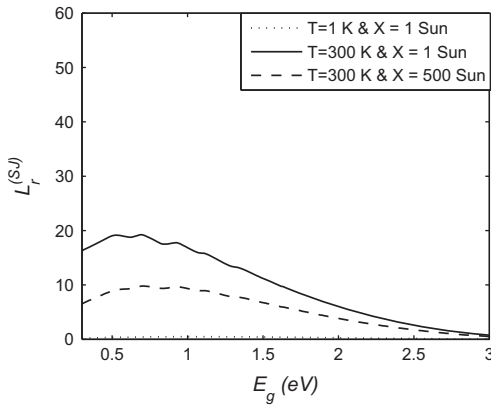

Fig. 11. $L_r^{(SJ)}$ vs. E_g for a single junction solar cell at different optical concentration and temperature.

3.2. Multi-cell devices

As shown in the previous section, more than 50% of energy is lost either due to thermalization or for not absorbed photons. This was known since the early days of solar cells [31,40,101,132] and many concepts were developed to regain the lost energy. The main concepts were discussion in Section 2. For many concepts like thermalization control and spectrum manipulation ones, there is no general way to estimate the practical efficiency limits. Some models are developed for them; but, they are not practical as they usually result in extreme over-estimation [118,136–138]. For
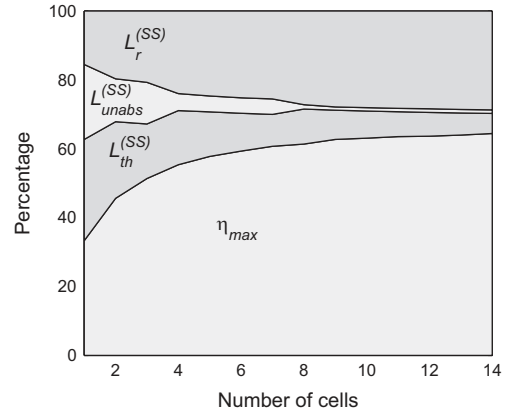

Fig. 12. The optimized η of split spectrum solar cell system for different number of cells at $T = 300$ K and with no carrier multiplication. The corresponding $L_{unabs}^{(SJ)}$, $L_{th}^{(SJ)}$, and $L_r^{(SJ)}$ for each E_g are added up.

multi-cell devices such as multi-junction and split spectrum, estimating the upper limit can be achieved by extending the single junction model.

Abstractly, in such devices, the spectrum is split and then different cells are used to convert the energy by matching E_g. So, there should be N cells with different $E_g^{(i)}$'s (the gaps are ordered ascendantly). Thus, the generated current in the ith cell is

$$J_g^{(i)} = q \int_{E_g^{(i)}}^{E_g^{(i+1)}} \gamma(E)\phi(E) \, dE \tag{11}$$

For the last cell, the upper limit goes to ∞. Similar to the case of single junction devices, the recombination current is calculated based on the generalized black body radiation and it is

$$J_r^{(i)} = qa \int_{E_g^{(i)}}^{\infty} \frac{E^2}{\exp\left(\dfrac{E - \gamma(E)V^{(i)}}{kT}\right) - 1} \, dE \tag{12}$$

So, the net generated current in the ith cell is

$$J^{(i)}(E_g, V, T) = J_g^{(i)} - J_r^{(i)} \tag{13}$$

Then for each cell, the conversion efficiency becomes

$$\eta^{(i)}(V^{(i)}) = \frac{V^{(i)}J^{(i)}}{P_{in}} \tag{14}$$

In split spectrum cells, the photo-generated current is extracted separately for each cell. So, the total efficiency is

$$\eta^{(SS)} = \sum_i \eta^{(i)} = \frac{1}{P_{in}} \sum_i V^{(i)} J^{(i)} \tag{15}$$

For multijunction and intermediate band cells, the photo-generated current should flow from one cell to the other before extracted in the external terminals. This series connection imposes that the current should be the same in all of used cells and it is equal to the lowest current achieved by any of the cells. Thus, the optimization becomes two-step problem. In the first one, $V^{(i)}$ is varied to optimize $\eta^{(i)}$ for each cell. Then the lowest achievable current J_{min} is maintained and hence the $V^{(i)}$ and $\eta^{(i)}$ are changed accordingly. This is done iteratively to maximize the net efficiency which reads

$$\eta^{(MJ)} = \sum_i \eta^{(i)} = \frac{1}{P_{in}} J_{min} \sum_i V^{(i)} \tag{16}$$

At the beginning, η is optimized for operation at $T = 300$ K and with no carrier multiplication for different numbers of cells where E_g's are varied for optimization. Fig. 12 shows the results for split spectrum cell system and Fig. 13 shows the results for
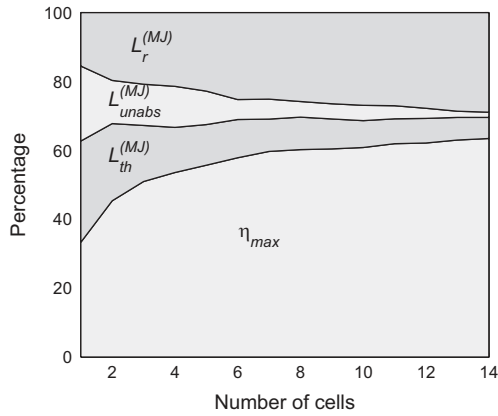
Fig. 13. The optimized η of multi-junction solar cells for different number of cells at $T = 300$ K and with no carrier multiplication. The corresponding $L_{unabs}^{(SJ)}$, $L_{th}^{(SJ)}$, and $L_{r}^{(SJ)}$ for each E_g are added up.
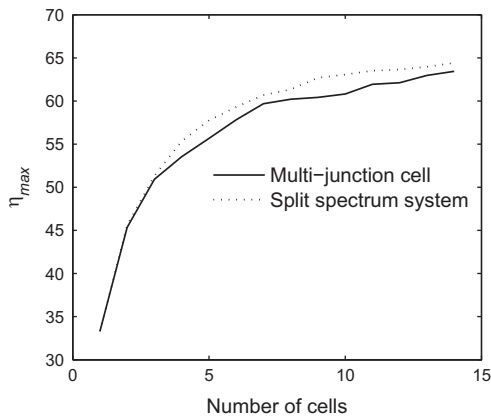

Fig. 14. η_{max} of multi-junction solar cells and split spectrum solar cell system for different number of cells at $T = 300$ K and with no carrier multiplication.

multi-junction cell, where the corresponding L_{unabs}, L_{th}, and L_r are calculated as well. As expected, η increases in both cases, but it is slightly better for split spectrum system as the constraint of current continuity is not a problem. This is shown clearly in Fig. 14. The difference in η_{max} between the two concepts is larger when the number of cells is between 4 and 12. The difference is then diminished for the unpractical larger number of cells. For very large number of cells, the theoretical η limit approaches 66%.

The concept of multi-cell devices was introduced to reduce L_{unabs} and L_{th}, which certainly get less with the number of cells. On the other hand, L_r increases considerably. This is because the gained energy by reducing L_{unabs} and L_{th} effects is distributed between the extracted photo-generated and radiatively recombined carriers.

3.3. Thermalization control based devices

For thermalization control based devices, there is no general way to estimate efficiency limits as different concepts are applied to control (or avoid) thermalization. In the following, we will discuss the devices based on CM. To raise solar cell efficiencies beyond Shockley–Queisser limit, CM route is proposed [64,139–143]. As aforementioned, the concept of CM is that an energetic photon is utilized to generate multiple electron–hole pairs before it relaxes. Theoretically, many mechanisms can result in CM such as impact ionization [144,145], coherent superposition of multi-excitons [146,147], singlet fission [148,149], and multiexciton

generation through virtual states [150]. Actually, many of these mechanisms are highly correlated.

Experimentally, many groups demonstrate CM for both bulk and nanoscale semiconductor systems. The highest obtained multiplication is seven times in lead salt quantum dots (QDs) by Schaller and Klimov [106]. However, the experimental apparatuses in most CM experiments are very sophisticated and do not resemble practical PV operations. It is very common in such experiments to induce sequential absorption and force impact ionization by high excitation and strong bias voltage. The significance of CM and its applicability in solar cells are questioned by many [22,109]. Practically, results are irreproducible in many cases [107,108]. For example, Pijpers et al. [151] rebutted their own earlier results [152] that overvalued the measured CM. Also, to have significant enhancement in solar cells, CM should be almost ideal. Obviously, this is not the case and it is always noticed that there is an energy threshold preceding the multiplication and that the multiplication is not perfect. It has been shown that these facts limit almost completely any possible enhancement [22,109].

Conceptually, the ideal CM condition is when

$$\gamma(E) = \left[\frac{E}{E_g}\right] \tag{17}$$

where the square brackets represent rounding to the lower integer. By considering the fact that energy threshold (E_{th}) is always needed before CM starts. Then, the multiplication $\gamma(E)$ becomes

$$\gamma(E) = \theta(E - E_g) + \theta(E - E_{th})\left[\frac{E - E_{th} + E_g}{E_g}\right] \tag{18}$$

where θ is the Heaviside step function. Furthermore, CM is not perfect and the increase of γ over E/E_g is less than one. So, the multiplication would be

$$\gamma(E) = \theta(E - E_g) + \theta(E - E_{th})\left(\frac{E - E_{th}}{E_g}\right)\lambda \tag{19}$$

Many models have been used to estimate both E_{th} and λ. Alharbi [22] suggested using empirical relation extracted from experimental data to estimate E_{th}. This relation will be used in this review and it is

$$E_{th} = E_{th,0} + (1 + f)E_g \tag{20}$$

where both $E_{th,0}$ and f are positive. They are interpolated from experimental data to fit the measured E_{th} for different materials. Over solar radiation spectrum, the fitting should ensure that $E_{th} \geq 2E_g$. For lead salt, it is found that $E_{th,0} = 1.2565$ and $f = 0.3604$ for PbS and $E_{th,0} = 1.3493$ and $f = 0.4005$ for PbSe [22].

Figs. 15 and 16 show the optimized η and the corresponding L_{th} vs. E_g for different CM conditions; namely, No CM, Perfect CM, and the condition for PbS. The condition of PbS is used as its data is the best among the least controversial in terms of CM [153]. It can be observed that more improvement is obtainable for small E_g. This is mainly due to the fact that solar radiation start decaying at 3.0 eV and becomes negligible above 4.0 eV. So, CM becomes negligible for cells with $E_g > 2.0$ eV. Theoretically, the efficiency limit can be raised from 33.3% at $E_g = 1.14$ eV to 44.1% at $E_g = 0.71$ eV if CM is perfect. However and as aforementioned, this is practically very challenging and it is found that CM advantage for solar cells is severely limited by the needed energy threshold and the imperfect multiplication. To illustrate that, the condition of PbS is used. As can be seen from Fig. 15, the theoretical possible improvement is very marginal.

To illustrate the effects of the needed energy threshold and the imperfect multiplication, E_{th} and λ are changed slightly from the perfect condition. In Fig. 17, $E_{th,0}$ is changed by varying f from 0 (perfect CM) to 2 at steps on 0.4 where $E_{th,0}$ is set to 1. It is clear
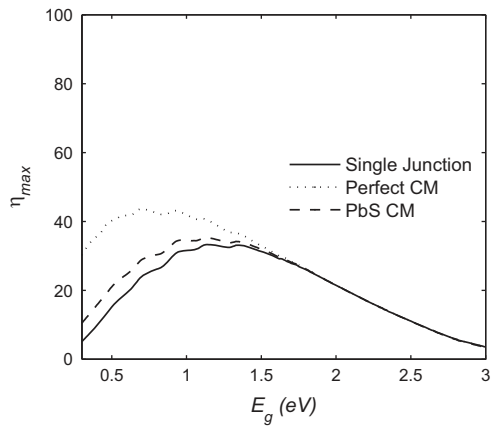
Fig. 15. The optimized η vs. E_g for different CM conditions; namely, No CM, Perfect CM, and the condition for PbS (to correct the legends).
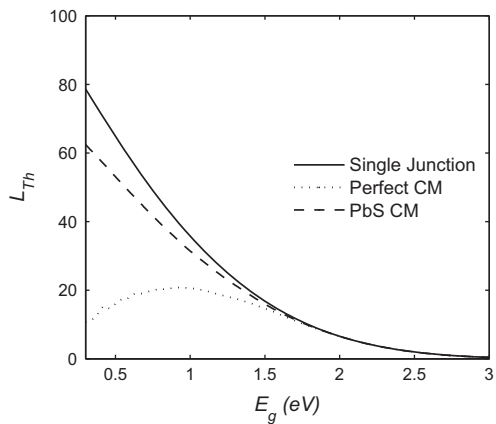

Fig. 16. The corresponding L_{th} for the optimized η vs. E_g for different CM conditions; namely, No CM, Perfect CM, and the condition for PbS (to correct the legends).

Fig. 17. The optimized η vs. E_g when $E_{th,0} = E_g$ and f is varied from 0 (perfect CM) to 2 at steps on 0.4 along the direction of the arrow.

Fig. 18. The optimized η vs. E_g when E_{th} is assumed perfect and equal to $2E_g$ and λ is varied 1 (perfect CM) to 0.2 at steps on 0.2 along the direction of the arrow.

that the advantage of CM is dying rapidly. This is even severer if the multiplication is assumed imperfect as shown in Fig. 18. In this figure, E_{th} is assumed perfect and equal to $2E_g$. λ is varied 1 (perfect CM) to 0.2 at steps on 0.2. η dyes very fast with decreasing λ.

4. Photosynthesis: solar-to-chemical energy conversion

Sunlight is the most abundant energy source available on earth, and therefore designing systems that can effectively gather, transfer, or store solar energy has been a great continuing challenge for researchers. To achieve this, a very intuitive approach is to learn from Mother Nature. In light harvesting organisms, the major mechanism that converts light energy into chemical energy is photosynthesis. Photosynthesis can be described by the simplified chemical reaction to obtain carbohydrates:

$$6CO_2 + 6H_2O + Nh\nu \rightarrow C_6H_{12}O_6 + 6O_2. \tag{21}$$

Estimates of the efficiency of photosynthesis have a long history [154–163] and depend on how light energy is defined. Ross and Hsiao [164] reported that the efficiency cannot exceed 29% based on an ideal theoretical analysis, where entropy and unavoidable irreversibility place a limit on the efficiency of photochemical solar energy conversion. However, photosynthesis is known to occur at $\lambda \leq 700$ nm, where only about 45% of the sun light is photosynthetically active. Based on these facts, Bolton and Hall [165] calculated the theoretical maximum efficiency of conversion of light to stored chemical energy in green-plant type photosynthesis in
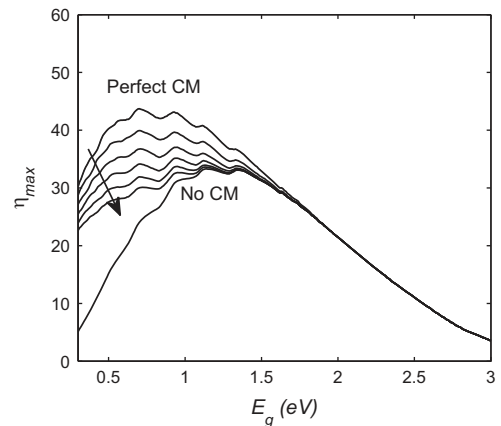
bright sunlight to be 13.0%, when the principal stable product of photosynthesis is d-glucose. Thermodynamic arguments used in the analysis which indicate that a photosynthetic system with one photosystem would be highly unlikely to be able to drive each electron from water to evolve O_2 and reduce CO_2. The practical maximum efficiency of photosynthesis under optimum conditions is estimated to be negligible, about few percents 1–3%.

Remarkably, in plants, bacteria, and algae, the photon-to-charge conversion efficiency is about 100% under certain conditions [11]. This fact is of great interest and generate a lot of excitement to understand how nature optimized the different molecular processes such as trapping, radiative, and non-radiative losses, and in particular the role of quantum coherence to enhance transport in photosynthesis. This might lead to allow engineering new materials mimicking photosynthesis and could be used to achieve similar performances in artificial solar cells [15,16]. Before discussing in detail the energy transfer in photosynthesis, first we introduce briefly the concept of quantum coherence which has ignited interest in the possible biological function after the experimental observation of coherence oscillations during energy transfer [166].

4.1. Quantum coherence

In photosynthetic light-harvesting complexes, the electronic coupling between chromophores is similar in magnitude to coupling to

the environment and to the disorder in site energies. Thus, quantum effects might influence the dynamics in these systems. It is common to examine dynamics of energy transfer in terms of the population evolution from one chromophore to another or from one site to another. Quantum coherence introduces correlations among wave function amplitudes at different sites. The full dynamics should include both the population evolution and coherence accounting for quantum superpositions. In the density matrix formulation, populations described by the diagonal elements and coherence by the off-diagonal elements.

A quantum state described by a density matrix ρ is called pure if it can be represented by a wave function Ψ, $\rho = |\Psi\rangle\langle\Psi|$, and mixed otherwise. The off-diagonal elements of the density matrix ρ are usually called coherences but they are basis-dependent. To illustrate the concept, let us focus on a system of two excitons described by $\Psi(t) = a\Phi_a + b\Phi_b$. The time evolution of the density matrix, $\rho(t) = |\Psi(t)\rangle\langle\Psi(t)|$, is given by

$$\rho(t) = |a|^2|\Phi_a\rangle\langle\Phi_a| + |b|^2|\Phi_b\rangle\langle\Phi_b| + ab^* e^{-i(E_a - E_b)t/\hbar}|\Phi_a\rangle\langle\Phi_b|$$
$$+ a^*b e^{+i(E_a - E_b)t/\hbar}|\Phi_b\rangle\langle\Phi_a|. \tag{22}$$

The first two diagonal terms represent populations in the excitonic basis, whereas the latter two off-diagonal describe coherences. The phase factors in the off-diagonal elements are responsible for quantum beating. The frequency of this beating corresponds to the energy difference between the two excitons giving information about the coherence between different chromophores. Recently, Kassal et al. [167], in order to address the question if coherence enhances transport in photosynthesis, introduce the distinction between state coherence and process coherence. They argue that although some photosynthetic pathways are partially coherent processes, photosynthesis in nature proceeds through stationary states [167].

4.2. Photosynthesis

In photosynthesis, the sunlight is absorbed and excites the electronic states of pigments in the antenna complexes. These electronic excitations then propagate to the reaction center and induce an electron transfer to the primary electron–acceptor molecular called pheophytin. This light to charge conversion is highly efficient and thus illustrates the importance of understanding this excitation energy transfer process in light-harvesting complexes (LHC).

Many light harvesting microbes such as green sulfur bacteria and purple bacteria have been studied as model organisms of photosynthesis. For example, in green sulfur bacteria the most commonly studied LHC is the Fenna–Matthews–Olson (FMO) complex. The FMO complex is situated between the antenna and the reaction center and functions as an energy pipeline between the two. If the excitonic energy transfer in such LHC can be understood thoroughly, it will be possible to design an artificial light-harvesting system with high efficiency based on a similar mechanism.

Recent experimental results show that long-lived quantum coherence is present in various photosynthetic complexes [168–170]. One such protein complex, the FMO complex from green sulphur bacteria [171,172], has attracted considerable experimental and theoretical attention due to its intermediate role in energy transport. The FMO complex plays the role of a molecular wire, transferring the excitation energy from the LHC to the reaction center (RC) [173–175]. Long-lasting quantum beating over a time scale of hundreds of femtoseconds has been observed [166,176]. The theoretical framework for modelling this phenomenon has also been explored intensively by many authors [177–202].

The fundamental physical mechanisms of energy transfer in photosynthetic complexes are not yet fully understood. In particular, the role of surrounding photonic and phononic environment on the efficiency or sensitivity of these systems for energy transfer. One major problem in studying LHCs has been the lack of an efficient method for simulating their dynamics under realistic conditions, in biological environments. There are mainly three methods to study the dynamics of such complex open quantum system:

1. The semiclassical Forster method in which the electronic Coulomb interaction among the different chromophores is treated perturbatively.
2. The Redfield or Lindblad method in which the electron–phonon interaction is treated perturbatively.
3. The Hierarchy equation of motion method for the intermediate regime when the strength of the Coulomb and electron–phonon interactions are comparable [192].

The full dynamics cannot be treated in such complex systems, thus people rely on simple model Hamiltonians interacting with an approximate environment. The total system Hamiltonian can be simplified and written as

$$H_{total} = H_S + H_B + H_{SB} \tag{23}$$

where the Hamiltonian for the system is

$$\mathcal{H}_S = \sum_{j=1}^{N} \varepsilon_j |j\rangle\langle j| + \sum_{j \neq k} J_{jk}(|j\rangle\langle k| + |k\rangle\langle j|), \tag{24}$$

where ε_j represents the excitation energy of the jth chromophore (site) and J_{jk} denotes the excitonic coupling between sites j and k. The non-nearest neighbor coupling between j and k is treated by the dipole–dipole interaction.

The environment is described as a phonon bath, modelled by an infinite set of harmonic oscillators:

$$\mathcal{H}_B = \sum_{j=1}^{N} \mathcal{H}_B^j = \sum_{j=1}^{N} \sum_{\xi=1}^{N_{jB}} \frac{P_{j\xi}^2}{2m_{j\xi}} + \frac{1}{2} m_{j\xi} \omega_{j\xi}^2 x_{j\xi}^2, \tag{25}$$

where $m_{j\xi}$, $\omega_{j\xi}$, $P_{j\xi}$, $x_{j\xi}$ are mass, frequency, momentum and position operator of the ξth harmonic bath associate with the jth site respectively.

The Hamiltonian of the environment ($\mathcal{H}_B$) and system–environment coupling ($\mathcal{H}_{SB}$) can be written as

$$\mathcal{H}_{SB} = \sum_{j=1}^{N} \sum_{\xi} c_{j\xi} |j\rangle\langle j| x_{j\xi} = \sum_{j=1}^{N} \mathcal{V}_j F_j, \tag{26}$$

where $\mathcal{V}_j = |j\rangle\langle j|$ and $F_j = \sum_{\xi} c_{j\xi} x_{j\xi}$. Here, $c_{j\xi}$ represents the system–bath coupling constant between the jth site and ξth phonon mode, here we assume that each site is coupled to the environment independently. The dynamics of such an open quantum system is given by the quantum Liouvillian equation and one has to rely on approximations depending on the different coupling terms.

To examine quantum coherence, Jing et al. [182] used a new developed modified scaled hierarchical approach, based on the model Hamiltonian defined above in Eq. (23), and show that the time scales of the coherent beating are consistent with experimental observations [166]. Furthermore, the theoretical results exhibit population beating at physiological temperature. Additionally, the method does not require a low-temperature correction to obtain the correct thermal equilibrium at long times. The results for the FMO complex are presented in Fig. 19. On the left panel, we show the results of simulation for the system Hamiltonian only. The right panel shows that the quantum beating between certain sites clearly persists in the short time dynamics of the full FMO complex [182,201]. For the simulated initial conditions, the
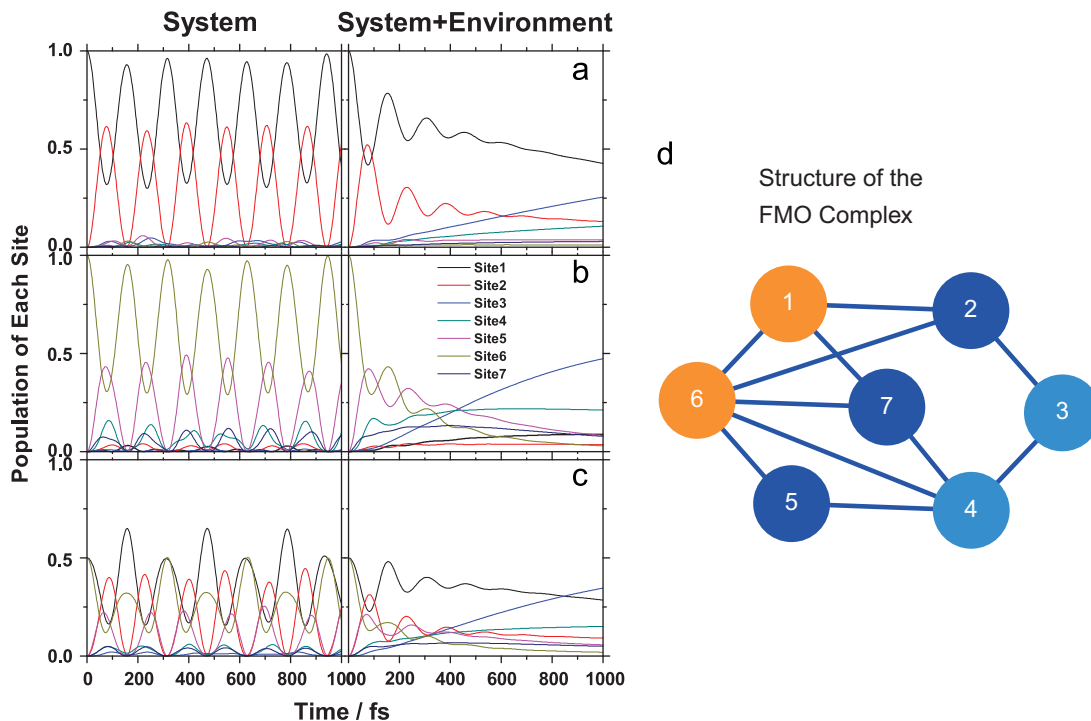
Fig. 19. The quantum evolution for the site population in the FMO complex of each site at cryogenic temperature $T = 77$ K. The left panel shows the dynamics for the system alone and the right includes the effects of the environment. The reorganization energy is $\lambda_j = \lambda = 35$ cm^1, while the value of Drude decay constant is $\gamma_j^{-1} = \gamma^{-1} = 50$ fs. The initial conditions are site 1 excited (a), site 6 excited (b) and the superposition of sites 1 and 6 (c).

population beatings can last for hundreds of femtoseconds; this time scale is in agreement with the experimental observation [166].

Recently, the modified scaled hierarchical approach was used also by Shuhao et al. [200] to examine the electronic excitation population and coherence dynamics in the chromophores of the photosynthetic light harvesting complex (LH2) B850 ring from purple bacteria (Rhodopseudomonas acidophila). The oscillations of the excitation population and coherence in the site basis are also observed in LH2. However, this oscillation time (300 fs) is much shorter compared to the FMO protein (650 fs) at cryogenic temperature. Both environment and high temperature are found to enhance the propagation speed of the exciton wave packet yet as expected they shorten the coherence time and suppress the oscillation amplitude of coherence and the population. In Fig. 20 we show the numerical results of the excitation population dynamics for LH2 B850 18 sites at 77 K.

Here we are dealing with exciton transport; excitons are quasiparticles, each formed from a pair of electron and hole, that provides a natural mean to convert energy between photons and electrons. There are several possible ways to measure the success rate of an energy transfer process [203], such as energy transfer efficiency and transfer time. In order to examine the transport efficiency one should calculate the exciton recombination and exciton trapping. These can be calculated by [203]

$$H_{trap} = -i\hbar \sum_j \kappa_j |j\rangle\langle j|; \quad H_{recomb} = -i\hbar \Gamma \sum_j |j\rangle\langle j| \qquad (27)$$

where Γ is the rate of recombination at every site and is trapped with a rate κ_j at certain molecules. The probability that the exciton is captured at a certain jth site within the time interval $(t, t+dt)$ is given by $2\kappa_j\langle j|\rho(t)|j\rangle \, dt$. Thus, the efficiency can be defined as

$$\eta = 2\sum_j \kappa_j \int_0^\infty \langle j|\rho(t)|j\rangle \, dt \qquad (28)$$

which is the integrated probability at different sites. The other measure for the quantum transport is the average transfer time

which is defined as

$$\tau = \frac{2}{\eta}\sum_j \kappa_j \int_0^\infty \langle j|\rho(t)|j\rangle t \, dt \qquad (29)$$

Recently, Rebentrost et al. [203] have argued that at low temperatures, the dynamic is dominated by coherent hopping, the system is disordered and exhibits quantum localization, depending on the variation in the site energies. Once forming an excitonic state localized at an initial site, coherent hopping alone has a low efficiency in transporting the excitation from the initial site to another site with significantly different energy. However, interaction with the environment leading to dephasing can destroy the excitation localization and enhance transport. Thus, decoherence might enhance transport if the dephasing rate does not grow larger than the terms of the system Hamiltonian. The idea that decoherence enhance transport used to explain the high efficiency of excitonic transport using FMO protein of the green sulfur bacterium [203].

4.2.1. Limits of quantum speedup in photosynthesis

After discovering experimentally the long lived quantum coherence in photosynthetic LHCs, it was suggested that excitonic transport features speedup analogous to those found in quantum algorithms; in particular, a Grover quantum search type speedup [166]. Whaley et al. [204] investigated this suggestion by comparing the dynamics in these systems to the dynamics of quantum walks. They have found that the speedup happens at very short time scale (70 fs) compared with the longer-lived quantum coherence (ps scale). To distinguish between quantum speedup and classical diffusive transport one can calculate the exponent, n, of the power law for the mean-squared displacement $\langle x^2 \rangle$ as a function of time, t. The mean-squared displacement can be obtained from the density matrix ρ of the system, $\langle x^2 \rangle = \text{Tr}(\rho x^2)/\text{Tr}(\rho)$. To obtain the exponent n in $\langle x^2 \rangle \approx t^n$, one examine the slope of the log–log plot of the mean-squared disparagement vs. time. If the exponent
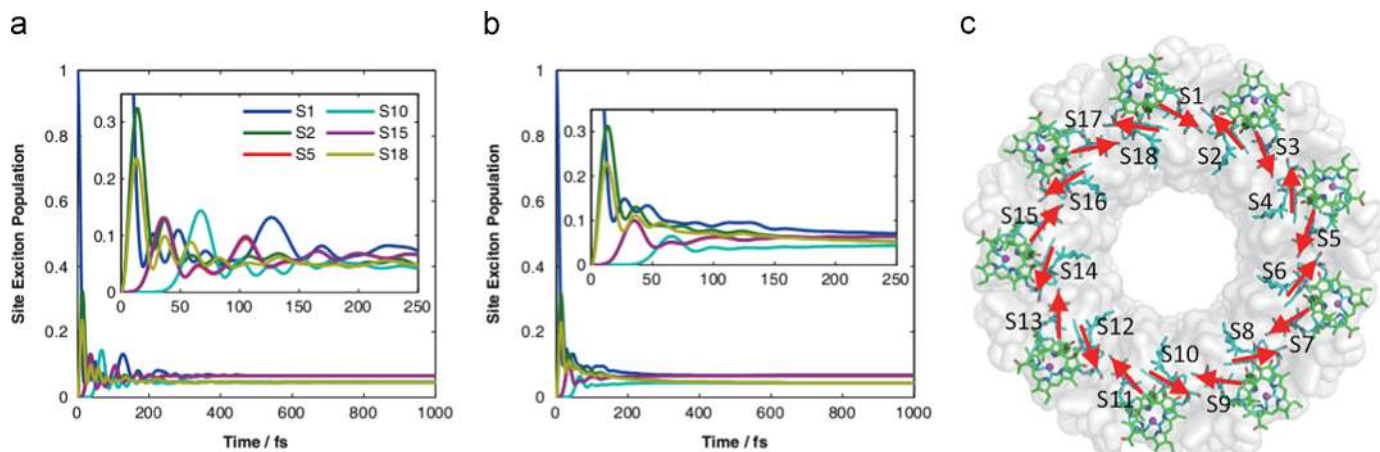
Fig. 20. The excitation population dynamics of LH2 B850 18 sites at 77 K. The exciton population dynamics of B850 bacteriochlorophylls (BChls) with site 1 (S1) initially excited. (a) The population evolution of S1, S2, S5, S10, S15, and S18 without dissipation (the system is isolated and uncoupled to bath). (b) The population dynamics of the same sites while the system is coupled to bath at room temperature $T=300$ K. The coherent energy transfer lasts about 150 fs and the whole system is equilibrated after 400 fs. The inset is a magnification of the first 250 fs dynamics.

$n=1$, this corresponds to the limit of diffusive transport, whereas the exponent $n=2$ corresponds to ideal quantum speedup, a ballistic transport. Using the FMO complex, which acts as a quantum wire, with a seven site Hamiltonian with the parameters calculated by Adolphs and Renger [205], Whaley et al. [204] have found that best fit for the exponent was $n=2$ happens at short time (about 70 fs), then a transition from ballistic to sub-diffusive transport with $n=1$ though quantum coherence lasts over 500 fs in their model of calculations. The short lived nature of quantum speedup (about 70 fs) might implies that the natural process of energy transfer in these photosynthetic complexes does not correspond to quantum search. Their results suggest that quantum coherence effects in photosynthetic complexes are optimized for high efficiency of transporting the excitation from the antenna to the reaction center and not for the goal of quantum speedup.

4.2.2. Excitonic diffusion length in complex quantum systems

It is well known that the phenomenon of superradiance, introduced by Dike [206], is formed by a quantum interference effect induced by symmetry. Due to this cooperative phenomena, the probability of a single photon emission from N identical atoms collectively interacting with vacuum fluctuations becomes N times larger than incoherent individual spontaneous emission probabilities [207]. This is studied in detail in [208–211]. The same basic mechanism could lead to an analogous phenomenon known as cooperative energy transfer or supertransfer [212–214], in particular, the exciton transfer rate under such assumptions. With very strong and symmetrized interactions of N molecules the excitation becomes highly delocalized, leading to a large effective dipole moment associated with the N molecules, and hence leading to supertransfer. Abasto et al. [215] have shown that symmetric couplings among aggregates of N chromophores increase the transfer rate of excitons by a factor N^2 and demonstrated how supertransfer effects induced by geometrical symmetries can enhance the exciton diffusion length by a factor N along cylindrically symmetric structures, consisting of arrays of rings of chromophores, and along spiral arrays. It will be of great interest to examine this phenomena in novel excitonic devices since a major problem in their designs and fabrications is the limited exciton diffusion length that could be of about 10 nm in disordered materials. This limitation has lead to low efficiency and complicated device structures in OPVs [216]. It will be of interest to examine whether one can use quantum-mechanical supertransfer effects to enhance exciton diffusion length in PVs [216–218].

5. Quantum coherence: intuitive aspects for solar energy conversion

Quantum mechanics which was developed in the twentieth century continues to yield new fruit in the twenty-first century. For example, quantum coherence effects such as lasing without inversion [17,18], the Photo-Carnot Quantum heat engine [19], Photosynthesis, and the quantum photocell [20] are topics of current research interest which are yielding new insights into thermodynamics and optics.

Photosynthesis is one of the most common phenomenon in nature, but the detailed principles of the whole process are still unclear. A more recent and still rapidly expanding field of research studies how quantum physics plays a much more profound role in solar-energy conversion, notably through various interference and coherence effects. The energy transfer from the LHC to the RC is amazingly high, almost 100%. Does quantum coherence enhance transport in photosynthesis? Artificially reproducing the biological light reactions responsible for this remarkably efficiency represents a new research direction. Recently, Creatore et al. [16] developed such a scheme and presented a model photocell based on the nanoscale architecture of photosynthetic reaction centers that explicitly harnesses the quantum mechanical effects recently discovered in photosynthetic complexes. They show that Quantum interference of photon absorption/emission induced by the dipole–dipole interaction between molecular excited states, as shown in Fig. 21, guarantees an enhanced light-to-current conversion and hence power generation for a wide range of realistic parameters. The enhancement in the current is shown in Fig. 22. This shall open a promising new route for designing artificial light-harvesting devices inspired by biological photosynthesis and quantum technologies. They show that the naturally occurring dipole–dipole interactions between suitably arranged chromophores can generate quantum interference effects that can enhance the photo-currents and maximum power outputs by $>35\%$ over a classical cell.

Quantum heat engines convert hot thermal radiation into low-entropy useful work. The ultimate efficiency of such system is usually governed by a detailed balance between absorption and emission of the hot pump radiation. The laser is an example of
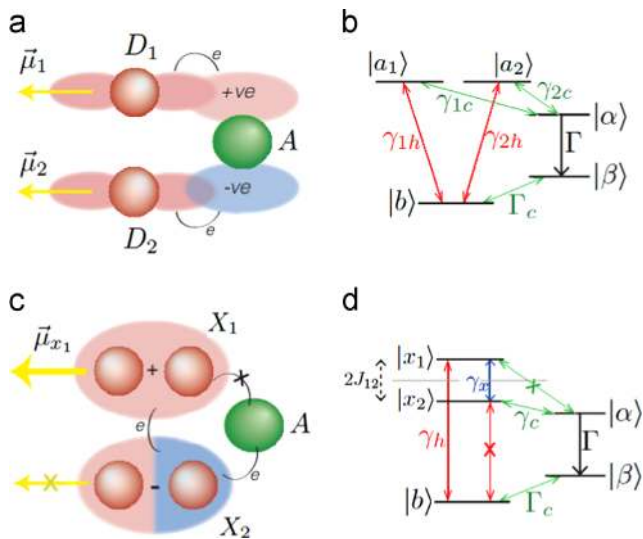
Fig. 21. The photosynthetic reaction centers used in the scheme proposed by Creatore et al. [16] to enhance photon to current conversion by suppressing the recombination. In (a), the doners D_1 and D_2 are identical, but uncoupled. In this case, the recombination is not suppressed and the rates γ_{1h} and γ_{2h} are equal. (b) is the level scheme of this case. In (c), the coupling between the doners results in coupled eigenstates (X_1 and X_2) due to the symmetric and antisymmetric superposition of the original doner states. The level scheme of this system is shown in (d). The analysis shows that recombination is suppressed as a result of the coupling (copied with permission from the original paper: PRL 111, 253601 (2013) [16]).
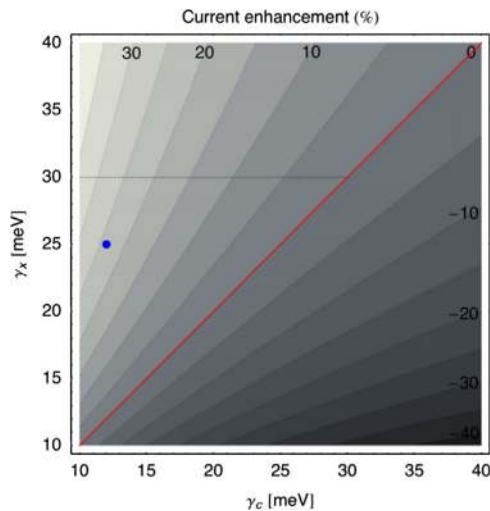

Fig. 22. The current enhancement due to coupling between the original doners as a function of various relaxation rate (γ_x) and the electron transfer rate (γ_c) at 300 K (copied with permission from the original paper: PRL 111, 253601 (2013) [16]).

such system. Moreover, it was demonstrated both theoretically and experimentally that noise-induced quantum coherence can break detailed balance and yield lasers without population inversion with enhanced efficiency [219]. Scully shows [20] that it is possible to break detailed balance via quantum coherence which yields a quantum limit to photovoltaic operation which can exceed the classical Shockley–Quiesser limit. The analysis considers a toy photocell model which is constructed to be a counterpart to "lasing without inversion" . In conventional lasing, one considers an ensemble of two-level atoms (plus additional levels not directly involved in the photoemission process) all coupled to the same cavity mode. These atoms can undergo both absorption as well as the converse emission processes. If, by optical pumping, one achieves a situation in which there are more atoms in the excited than in the ground state (a so-called *inversion*) then emission will dominate over absorption, and one will under certain conditions observe a net emission, i.e., lasing. The idea is to relax the lasing threshold by suppressing the absorption process. This is achieved by splitting the atoms' ground state into two near-degenerate levels. In quantum mechanics, one cannot simply add the absorption probabilities for these two levels; instead, one has to add the relevant transition amplitudes coherently, and the resulting absorption rate may actually be *less* than the individual rates due to destructive interference. In an elegant corollary, one can now try to suppress the *emission* process in a photovoltaic device (which in this case is the undesirable process, leading to efficiency loss via recombination), by replacing the *upper* level with a near-degenerate doublet, engineering the system parameters such that the two recombination sub-processes interfere destructively. Recently, Dorfman et al. [219] have introduced a promising approach to this problem, in which the light reactions are analyzed as quantum heat engines. Treating the light-to-charge conversion as a continuous Carnot like cycle they show that quantum coherence could boost the photo-current of a photocell based on photosynthetic reaction centers by at least 27% compared to an equivalent classical photocell.

Two seemingly unrelated effects attributed to quantum coherence have been discussed. First, an enhanced solar cell efficiency was predicted and second, population oscillations were measured in photosynthetic antennae excited by sequences of coherent ultrashort laser pulses. Both systems operate as quantum heat engines that convert the solar photon energy to chemical energy in photosynthesis and to electric current in solar cells. Artificially reproducing the biological light reactions responsible for the remarkably efficient photon-to-charge conversion in photosynthetic complexes represents a new direction for the future development of photovoltaic devices.

6. Conclusion

In this review, we summarized different PV device concepts and their efficiency theoretical limits where more discussion emphasize is toward the losses. It is shown that the efficiency of single-junction PV is at best 33.3% in normal conditions at 300 K. This can be improved by either cooling or optical concentration to 48.48% and 40%+ respectively. However, optical concentration is more practical. Cooling toward very low temperatures is not practical; yet, it can be conceptually mimicked. For multi-cell PV systems, the efficiency can be improved by reducing the losses due to thermalization and unabsorbed photons. The analysis shows that split-spectrum system should result in better efficiency when compared to multijunction and intermediate cells. Though bulky, it is easier to build.

Few lessons from nature and other fields to improve the conversion efficiency in PVs are presented and discussed. From photosynthesis, although it was shown that the whole conversion efficiency of photosynthesis process is not compelling, the perfect exciton transport in photosynthetic complexes can be utilized for PVs. Remarkably, in plants, bacteria, and algae, the photon-to-charge conversion efficiency is about 100% under certain conditions. Also, we present some lessons learned from other field that can be used in PVs like recombination suppression by quantum coherence. For example, the coupling in photosynthetic reaction centers is used to suppress recombination in photocells. Theoretically, it can enhance the net photo-generated current by 35%.

References

[1] Adams WG, Day R. The action of light on selenium. Proc R Soc Lond 1876;25 (171–178):113–7.
[2] Dimroth F. World record solar cell with 44.7 ⟨http://www.ise.fraunhofer.de/en/press-and-media/press-releases/presseinformationen-2013/world-record-solar-cell-with-44.7-efficiency⟩, September 2013.
[3] Jäger-Waldau A. Status of thin film solar cells in research, production and the market. Sol Energy 2004;77(6):667–78.
[4] Poortmans J, Arkhipov V. Thin film solar cells: fabrication, characterization and applications, Chichester: John Wiley & Sons; 2006.
[5] Heo JH, Im SH, Noh JH, Mandal TN, Lim C-S, Chang JA, et al. Efficient inorganic–organic hybrid heterojunction solar cells containing perovskite compound and polymeric hole conductors. Nat Photonics 2013;7(6):486–91.
[6] Jeon NJ, Lee J, Noh JH, Nazeeruddin MK, Gratzel M, Seok SI. Efficient inorganic–organic hybrid perovskite solar cells based on pyrene arylamine derivatives as hole-transporting materials. J Am Chem Soc 2013;135 (51):19087–90.
[7] Burschka J, Pellet N, Moon S-J, Humphry-Baker R, Gao P, Nazeeruddin MK, et al. Sequential deposition as a route to high-performance perovskite-sensitized solar cells. Nature 2013;499(7458):316–9.
[8] Liu M, Johnston MB, Snaith HJ. Efficient planar heterojunction perovskite solar cells by vapour deposition. Nature 2013;501(7467):395–8.
[9] Kojima A, Teshima K, Shirai Y, Miyasaka T. Organomethal halide perovskites as visible-light sensitizers for photovoltaic cells. J Am Chem Soc 2009;131 (17):6050–1.
[10] Green MA, Ho-Baillie A, Snaith HJ. The emergence of perovskite solar cells. Nat Photonics 2014;8(7):506–14.
[11] Blankenship RE. Molecular mechanisms of photosynthesis. Wiley.com; 2008.
[12] Blankenship RE, Tiede DM, Barber J, Brudvig GW, Fleming G, Ghirardi M, et al. Comparing photosynthetic and photovoltaic efficiencies and recognizing the potential for improvement. Science 2011;332(6031):805–9.
[13] Grätzel M. The artificial leaf, molecular photovoltaics achieve efficient generation of electricity from sunlight. Comments Inorg Chem 1991;12(2–3):93–111.
[14] Imahori H, Kashiwagi Y, Hasobe T, Kimura M, Hanada T, Nishimura Y, et al. Porphyrin and fullerene-based artificial photosynthetic materials for photovoltaics. Thin Solid Films 2004;451:580–8.
[15] Würfel P. Physics of solar cells: from basic principles to advanced concepts. Wiley.com; 2009.
[16] Creatore C, Parker M, Emmott S, Chin A. Efficient biologically inspired photocell enhanced by delocalized quantum states. Phys Rev Lett 2013;111:253601.
[17] Kocharovskaya O. Amplification and lasing without inversion. Phys Rep 1992;219(3):175–90.
[18] Scully M, Zubairy S. Quantum optics. Cambridge: Cambridge Press; 1997.
[19] Scully MO, Zubairy MS, Agarwal GS, Walther H. Extracting work from a single heat bath via vanishing quantum coherence. Science 2003;299(5608):862–4.
[20] Scully MO. Quantum photocell: using quantum coherence to reduce radiative recombination and increase efficiency. Phys Rev Lett 2010;104 (20):207701.
[21] Hanna M, Nozik A. Solar conversion efficiency of photovoltaic and photoelectrolysis cells with carrier multiplication absorbers. J Appl Phys 2006;100 (7):074510.
[22] Alharbi FH. Carrier multiplication applicability for photovoltaics; a critical analysis. J Phys D: Appl Phys 2013;46(12):125102.
[23] Becquerel A. Mémoire sur les effets électriques produits sous linfluence des rayons solaires. Comptes Rendus 1839;9(567):1839.
[24] Williams R. Becquerel photovoltaic effect in binary compounds. J Chem Phys 1960;32(5):1505–14.
[25] Weston E. Apparatus for utilizing solar radiant energy. US Patent 389,124; 1888.
[26] Weston E. Art of utilizing solar radiant energy. US Patent 389,125; 1888.
[27] Severy ML. Apparatus for mounting and operating thermopiles. US Patent 527,377; 1894.
[28] Severy ML. Apparatus for generating electricity by solar heat. US Patent 527,379; 1894.
[29] Chapin D, Fuller C, Pearson G. A new silicon p–n junction photocell for converting solar radiation into electrical power. J Appl Phys 1954;25 (5):676–7.
[30] Prince M, Wolf M. New developments in silicon photovoltaic devices. J Br Inst Radio Eng 1958;18(10):583–94.
[31] Loferski JJ. Theoretical considerations governing the choice of the optimum semiconductor for photovoltaic solar energy conversion. J Appl Phys 1956;27 (7):777–84.
[32] Wadia C, Alivisatos AP, Kammen DM. Materials availability expands the opportunity for large-scale photovoltaics deployment. Environ Sci Technol 2009;43(6):2072–7.
[33] Alharbi F, Bass JD, Salhi A, Alyamani A, Kim H-C, Miller RD. Abundant non-toxic materials for thin film solar cells: alternative to conventional materials. Renew Energy 2011;36(10):2753–8.
[34] Hossain M, Alharbi F. Recent advances in alternative material photovoltaics. Mater Technol: Adv Perform Mater 2013;28(1–2):88–97.
[35] Lux-Steiner MC. Non-conventional semiconductor materials for solar cells. Springer Proc Phys 1991;54:420–31.
[36] Curtright AE, Morgan MG, Keith DW. Expert assessments of future photovoltaic technologies. Environ Sci Technol 2008;42(24):9031–8.
[37] Yoo S-H, Butler KT, Soon A, Abbas A, Walls JM, Walsh A. Identification of critical stacking faults in thin-film cdte solar cells. Appl Phys Lett 2014;105 (6):062104.
[38] Jackson P, Hariskos D, Lotter E, Paetel S, Wuerz R, Menner R, et al. New world record efficiency for cu (in, ga) se2 thin-film solar cells beyond 20%. Prog Photovolt: Res Appl 2011;19(7):894–7.
[39] Shockley W, Queisser HJ. Detailed balance limit of efficiency of p–n junction solar cells. J Appl Phys 1961;32(3):510–9.
[40] Landsberg P, Tonge G. Thermodynamic energy conversion efficiencies. J Appl Phys 1980;51(7):R1–20.
[41] Prasad G, Srivastava O. The high-efficiency (17.1%) wse2 photoelectrochemical solar cell. J Phys D: Appl Phys 1988;21(6):1028.
[42] Pathak V, Srivastava R. Series resistance in n-mose$_2$ (tmdc)-based pec solar cells. Sol Energy 1993;50(2):123–7.
[43] Vogt M, Lux-Steiner M, Dolatzoglou P, Reetz W, Bumuller B, Bucher E. Improvement of wse 2 solar cells by doping?. In: Photovoltaic specialists conference. Conference record of the twenty first IEEE. IEEE, Kissimmee, FL; 1990. p. 519–24.
[44] Tang CW. Two-layer organic photovoltaic cell. Appl Phys Lett 1986;48 (2):183–5.
[45] Darling SB, You F. The case for organic photovoltaics. Rsc Adv 2013;3 (39):17633–48.
[46] Lizin S, Van Passel S, De Schepper E, Maes W, Lutsen L, Manca J, et al. Life cycle analyses of organic photovoltaics: a review. Energy Environ Sci 2013;6 (11):3136–49.
[47] Carlé JE, Krebs FC. Technological status of organic photovoltaics (opv). Sol Energy Mater Solar Cells 2013;119:309–10.
[48] Ameri T, Khoram P, Min J, Brabec CJ. Organic ternary solar cells: a review. Adv Mater 2013;25(31):4245–66.
[49] Service RF. Outlook brightens for plastic solar cells; 2011.
[50] Vlachopoulos N, Liska P, Augustynski J, Grätzel M. Very efficient visible light energy harvesting and conversion by spectral sensitization of high surface area polycrystalline titanium dioxide films. J Am Chem Soc 1988;110 (4):1216–20.
[51] Grätzel M. Dye-sensitized solar cells. J Photochem Photobiol C: Photochem Rev 2003;4(2):145–53.
[52] Grätzel M. Photoelectrochemical cells. Nature 2001;414(6861):338–44.
[53] Oregan B, Grätzel M. A low-cost, high-efficiency solar cell based on dye-sensitized. Nature 1991;353:737–40.
[54] Gerischer H, Michel-Beyerle M, Rebentrost F, Tributsch H. Sensitization of charge injection into semiconductors with large band gap. Electrochim Acta 1968;13(6):1509–15.
[55] Gerischer H. Electrochemical photo and solar cells principles and some experiments. J Electroanal Chem Interfacial Electrochem 1975;58(1):263–74.
[56] Osa T, Fujihira M. Photocell using covalently-bound dyes on semiconductor surfaces. Nature 1976;264:349.
[57] Fujihira M, Kubota T, Osa T. Organo-modified metal oxide electrode: part v. Efficiency of electron injection into conduction band from photo-excited dye molecule covalently attached to an sno2 surface. J Electroanal Chem Interfacial Electrochem 1981;119(2):379–87.
[58] Nickel B, Staerk H, Weller A. Energy transfer from adsorbed dye molecules to anthracene single crystals. Chem Phys Lett 1969;4(1):27–30.
[59] Knibbe H, Rehm D, Weller A. Intermediates and kinetics of fluorescence quenching by electron transfer. Ber Bunsenges Phys Chem 1968;72(2): 257–63.
[60] Nazeeruddin MK, De Angelis F, Fantacci S, Selloni A, Viscardi G, Liska P, et al. Combined experimental and dft-tddft computational study of photoelectrochemical cell ruthenium sensitizers. J Am Chem Soc 2005;127 (48):16835–47.
[61] Chung I, Lee B, He J, Chang RP, Kanatzidis MG. All-solid-state dye-sensitized solar cells with high efficiency. Nature 2012;485(7399):486–9.
[62] Wang H, Zhang X, Gong F, Zhou G, Wang Z-S. Novel ester-functionalized solid-state electrolyte for highly efficient all-solid-state dye-sensitized solar cells. Adv Mater 2012;24(1):121–4.
[63] Armel V, Forsyth M, MacFarlane DR, Pringle JM. Organic ionic plastic crystal electrolytes; a new class of electrolyte for high efficiency solid state dye-sensitized solar cells. Energy Environ Sci 2011;4(6):2234–9.
[64] Nozik A. Quantum dot solar cells. Physica E: Low-dimensional Syst Nanostruct 2002;14(1):115–20.
[65] Giménez S, Mora-Seró I, Macor L, Guijarro N, Lana-Villarreal T, Gómez R, et al. Improving the performance of colloidal quantum-dot-sensitized solar cells. Nanotechnology 2009;20(29):295204.
[66] Robel I, Subramanian V, Kuno M, Kamat PV. Quantum dot solar cells. Harvesting light energy with cdse nanocrystals molecularly linked to mesoscopic tio2 films. J Am Chem Soc 2006;128(7):2385–93.
[67] Kongkanand A, Tvrdy K, Takechi K, Kuno M, Kamat PV. Quantum dot solar cells. Tuning photoresponse through size and shape control of cdse-tio2 architecture. J Am Chem Soc 2008;130(12):4007–15.
[68] Kamat PV. Quantum dot solar cells. Semiconductor nanocrystals as light harvesters. J Phys Chem C 2008;112(48):18737–53.
[69] Mitzi DB. Synthesis, structure, and properties of organic–inorganic perovskites and related materials. Prog Inorgan Chem 2007;48:1–121.
[70] Mitzi DB. Templating and structural engineering in organic–inorganic perovskites. J Chem Soc Dalton Trans 2001;1(1):1–12.

[71] McGehee MD. Materials science: fast-track solar cells. Nature 2013;501 (7467):323–5.

[72] Snaith HJ. Perovskites: the emergence of a new era for low-cost, high-efficiency solar cells. J Phys Chem Lett 2013;4(21):3623–30.

[73] Carnie MJ, Charbonneau C, Davies ML, Troughton J, Watson TM, Wojciechowski K, et al. A one-step low temperature processing route for organolead halide perovskite solar cells. Chem Commun 2013;49(72):7893–5.

[74] Ball JM, Lee MM, Hey A, Snaith HJ. Low-temperature processed meso-superstructured to thin-film perovskite solar cells. Energy Environ Sci 2013;6(6):1739–43.

[75] Mitzi DB, Feild C, Harrison W, Guloy A. Conducting tin halides with a layered organic-based perovskite structure. Nature 1994;369:467–9.

[76] Mitzi D, Wang S, Feild C, Chess C, Guloy A. Conducting layered organic–inorganic halides containing ⟨110⟩−oriented perovskite sheets. Science 1995;267(5203):1473–6.

[77] Kagan C, Mitzi D, Dimitrakopoulos C. Organic–inorganic hybrid materials as semiconducting channels in thin-film field-effect transistors. Science 1999;286(5441):945–7.

[78] Mitzi DB, Chondroudis K, Kagan CR. Organic–inorganic electronics. IBM J Res Dev 2001;45(1):29–45.

[79] Luque A, Martí A, Nozik AJ. Solar cells based on quantum dots: multiple exciton generation and intermediate bands. Mrs Bull 2007;32(3):236–41.

[80] Sargent EH. Colloidal quantum dot solar cells. Nat Photonics 2012;6 (3):133–5.

[81] Adachi MM, Labelle AJ, Thon SM, Lan X, Hoogland S, Sargent EH. Broadband solar absorption enhancement via periodic nanostructuring of electrodes. Sci Rep 2013;3:2928.

[82] Kramer IJ, Sargent EH. The architecture of colloidal quantum dot solar cells: materials to devices. Chem Rev 2013;114(1):863–82.

[83] Huynh WU, Dittmer JJ, Alivisatos AP. Hybrid nanorod-polymer solar cells. Science 2002;295(5564):2425–7.

[84] Gur I, Fromer NA, Geier ML, Alivisatos AP. Air-stable all-inorganic nanocrystal solar cells processed from solution. Science 2005;310 (5747):462–5.

[85] Kim I, Lee TS, Jeong DS, Lee WS, Lee K-S. Size effects of metal nanoparticles embedded in a buffer layer of organic photovoltaics on plasmonic absorption enhancement. J Phys D: Appl Phys 2012;45(6):065101.

[86] Liang D, Kang Y, Huo Y, Chen Y, Cui Y, Harris JS. High-efficiency nanos-tructured window gaas solar cells. Nano Lett 2013;13(10):4850–6.

[87] Bozyigit D, Volk S, Yarema O, Wood V. Quantification of deep traps in nanocrystal solids, their electronic properties and their influence on device behavior. Nano Lett 2013;13(11):5284–8.

[88] Chuang C-HM, Brown PR, Bulović V, Bawendi MG. Improved performance and stability in quantum dot solar cells through band alignment engineering. Nat Mater 2014;13:796–801.

[89] Bett A, Dimroth F, Stollwerck G, Sulima O. Iii–v compounds for solar cell applications. Appl Phys A 1999;69(2):119–29.

[90] Yamaguchi M. Iii–v compound multi-junction solar cells: present and future. Sol Energy Mater Sol Cells 2003;75(1):261–9.

[91] Yamaguchi M, Takamoto T, Araki K, Ekins-Daukes N. Multi-junction iii–v solar cells: current status and future potential. Sol Energy 2005;79(1):78–85.

[92] Dimroth F. High-efficiency solar cells from iii–v compound semiconductors. Phys Status Solidi (c) 2006;3(3):373–9.

[93] Luque A, Martí A. Increasing the efficiency of ideal solar cells by photon induced transitions at intermediate levels. Phys Rev Lett 1997;78(26):5014.

[94] Luque A, Martí A. The intermediate band solar cell: progress toward the realization of an attractive concept. Adv Mater 2010;22(2):160–74.

[95] Martí A, Antolín E, Linares PG, Ramiro I, Artacho I, López E, et al. Six not-so-easy pieces in intermediate band solar cell research. J Photonics Energy 2013;3(1):031299.

[96] Wang W, Lin AS, Phillips JD. Intermediate-band photovoltaic solar cell based on znte: O. Appl Phys Lett 2009;95(1):011103.

[97] Martí A, Tablero C, Antolín E, Luque A, Campion R, Novikov S, et al. Potential of mn doped ln$_{1−x}$gaxn for implementing intermediate band solar cells. Sol Energy Mater Solar Cells 2009;93(5):641–4.

[98] Martí A, López N, Antolin E, Canovas E, Stanley C, Farmer C, et al. Novel semiconductor solar cell structures: the quantum dot intermediate band solar cell. Thin Solid Films 2006;511:638–44.

[99] Luque A, Marti A, Lopez N, Antolin E, Canovas E, Stanley C, et al. Experimental analysis of the quasi-Fermi level split in quantum dot intermediate-band solar cells. Appl Phys Lett 2005;87(8) 083505-083505.

[100] Shao Q, Balandin A, Fedoseyev A, Turowski M. Intermediate-band solar cells based on quantum dot supracrystals. Appl Phys Lett 2007;91(16):163503.

[101] Jackson E. Areas for improvement of the semiconductor solar energy converter. In: Transactions of the conference on the use of solar energy, vol. 5; 1955. p. 122–6.

[102] Moon R, James L, Vander Plas H, Yep T, Antypas G, Chai Y. Multigap solar cell requirements and the performance of algaas and si cells in concentrated sunlight. In: 13th Photovoltaic specialists conference, vol. 1; 1978. p. 859–67.

[103] Green MA, Ho-Baillie A. Forty three per cent composite split-spectrum concentrator solar cell efficiency. Prog Photovolt: Res Appl 2010;18(1):42–7.

[104] Hossain MI, Bousselham A, Alharbi FH. Optical concentration effects on conversion efficiency of a split-spectrum solar cell system. J Phys D: Appl Phys 2014;47(7):075101.

[105] Jackson ED. Solar energy converter. US Patent 2,949,498; August 16, 1960.

[106] Schaller RD, Sykora M, Pietryga JM, Klimov VI. Seven excitons at a cost of one: redefining the limits for conversion efficiency of photons into charge carriers. Nano Lett 2006;6(3):424–9.

[107] Pijpers J, Ulbricht R, Tielrooij K, Osherov A, Golan Y, Delerue C, et al. Assessment of carrier-multiplication efficiency in bulk pbse and pbs. Nat Phys 2009;5(11):811–4.

[108] Beard MC, Midgett AG, Law M, Semonin OE, Ellingson RJ, Nozik AJ. Variations in the quantum efficiency of multiple exciton generation for a series of chemically treated pbse nanocrystal films. Nano Lett 2009;9 (2):836–45.

[109] Takeda Y, Motohiro T. Requisites to realize high conversion efficiency of solar cells utilizing carrier multiplication. Sol Energy Mater Sol Cells 2010;94 (8):1399–405.

[110] Green MA. Third generation photovoltaics: solar cells for 2020 and beyond. Physica E: Low-dimensional Syst Nanostruct 2002;14(1):65–70.

[111] Le Bris A, Guillemoles J-F. Hot carrier solar cells: achievable efficiency accounting for heat losses in the absorber and through contacts. Appl Phys Lett 2010;97(11):113506.

[112] Würfel P, Brown A, Humphrey T, Green M. Particle conservation in the hot-carrier solar cell. Prog Photovolt: Res Appl 2005;13(4):277–85.

[113] Conibeer G, Jiang C-W, König D, Shrestha S, Walsh T, Green M. Selective energy contacts for hot carrier solar cells. Thin Solid Films 2008;516 (20):6968–73.

[114] Conibeer G, König D, Green M, Guillemoles J. Slowing of carrier cooling in hot carrier solar cells. Thin Solid Films 2008;516(20):6948–53.

[115] Gabor NM, Song JC, Ma Q, Nair NL, Taychatanapat T, Watanabe K, et al. Hot carrier-assisted intrinsic photoresponse in graphene. Science 2011;334 (6056):648–52.

[116] Song JC, Rudner MS, Marcus CM, Levitov LS. Hot carrier transport and photocurrent response in graphene. Nano Lett 2011;11(11):4688–92.

[117] Sun D, Aivazian G, Jones AM, Ross JS, Yao W, Cobden D, et al. Ultrafast hot-carrier-dominated photocurrent in graphene. Nat Nanotechnol 2012;7 (2):114–8.

[118] Abrams ZR, Gharghi M, Niv A, Gladden C, Zhang X. Theoretical efficiency of 3rd generation solar cells: comparison between carrier multiplication and down-conversion. Sol Energy Mater Sol Cells 2012;99:308–15.

[119] Verma D, Saetre TO. Midtgard O-M. Review on up/down conversion materials for solar cell application. In: Photovoltaic specialists conference (PVSC), 2012 38th IEEE. IEEE, Austin, TX; 2012. p. 002608–13.

[120] Coutts T. A review of progress in thermophotovoltaic generation of electricity. Renew Sustain Energy Rev 1999;3(2):77–184.

[121] Coutts TJ. An overview of thermophotovoltaic generation of electricity. Sol Energy Mater Sol Cells 2001;66(1):443–52.

[122] Bauer T. Thermophotovoltaics: basic principles and critical aspects of system design. Berlin: Springer; 2011.

[123] Datas A, Algora C. Development and experimental evaluation of a complete solar thermophotovoltaic system. Prog Photovolt: Res Appl 2013;21: 1025–39.

[124] Datas A, Algora C. Global optimization of solar thermophotovoltaic systems. Prog Photovolt: Res Appl 2013;21:1040–55.

[125] Davies P, Luque A. Solar thermophotovoltaics: brief review and a new look. Sol Energy Mater Sol Cells 1994;33(1):11–22.

[126] Badescu V. Upper bounds for solar thermophotovoltaic efficiency. Renew Energy 2005;30(2):211–25.

[127] Andreev V, Khvostikov V, Khvostikova O, Rumyantsev V, Gazarjan P, Vlasov A. Solar thermophotovoltaic converters: efficiency potentialities. In: AIP conference proceedings, vol. 738; 2004. p. 96–104.

[128] Fingerhut BP, Zinth W, de Vivie-Riedle R. The detailed balance limit of photochemical energy conversion. Phys Chem Chem Phys 2010;12 (2):422–32.

[129] De Vos A. Detailed balance limit of the efficiency of tandem solar cells. J Phys D: Appl Phys 1980;13(5):839.

[130] Bremner SP, Corkish R, Honsberg CB. Detailed balance efficiency limits with quasi-Fermi level variations [qw solar cell]. IEEE Trans Electron Devices 1999;46(10):1932–9.

[131] Brown AS, Green MA. Detailed balance limit for the series constrained two terminal tandem solar cell. Physica E: Low-dimensional Syst Nanostruct 2002;14(1):96–100.

[132] Landsberg P, Baruch P. The thermodynamics of the conversion of radiation energy for photovoltaics. J Phys A: Math Gen 1989;22(11):1911.

[133] Luque A, Martí A. Entropy production in photovoltaic conversion. Phys Rev B 1997;55(11):6994.

[134] Standard tables for reference solar spectral irradiances: direct normal and hemispherical on 37 tilted surface. Technical report, American Society for Testing and Materials ⟨http://www.astm.org/Standards/G173.htm ⟩, 2012.

[135] Riordan C, Hulstron R. What is an air mass 1.5 spectrum?. In: Photovoltaic specialists conference. Conference Record of the Twenty First IEEE. IEEE, Kissimmee, FL; 1990. p. 1085–8.

[136] Trupke T, Green M, Wurfel P. Improving solar cell efficiencies by down-conversion of high-energy photons. J Appl Phys 2002;92(3):1668–74.

[137] Shpaisman H, Niitsoo O, Lubomirsky I, Cahen D. Can up-and down-conversion and multi-exciton generation improve photovoltaics? Sol Energy Mater Sol Cells 2008;92(12):1541–6.

[138] van Sark W, Meijerink A, Schropp R, Van Roosmalen J, Lysen E. Enhancing solar cell efficiency by using spectral converters. Sol Energy Mater Sol Cells 2005;87(1):395–409.

[139] Kolodinski S, Werner JH, Wittchen T, Queisser HJ. Quantum efficiencies exceeding unity due to impact ionization in silicon solar cells. Appl Phys Lett 1993;63(17):2405–7.

[140] Kolodinski S, Werner JH, Queisser HJ. Quantum efficiencies exceeding unity in silicon leading to novel selection principles for solar cell materials. Sol Energy Mater Sol Cells 1994;33(3):275–85.

[141] Werner JH, Brendel R, Oueisser H. New upper efficiency limits for semi-conductor solar cells. In: IEEE first world conference on photovoltaic energy conversion. Conference record of the twenty fourth IEEE photovoltaic specialists conference-1994, vol. 2. IEEE, Waikoloa, HI; 1994. p. 1742–5.

[142] Würfel P. Solar energy conversion with hot electrons from impact ionisation. Sol Energy Mater Sol Cells 1997;46(1):43–52.

[143] De Vos A, Desoete B. On the ideal performance of solar cells with larger-than-unity quantum efficiency. Sol Energy Mater Sol Cells 1998;51(3):413–24.

[144] Franceschetti A, An J, Zunger A. Impact ionization can explain carrier multiplication in pbse quantum dots. Nano Lett 2006;6(10):2191–5.

[145] Luo J-W, Franceschetti A, Zunger A. Carrier multiplication in semiconductor nanocrystals: theoretical screening of candidate materials based on band-structure effects. Nano Lett 2008;8(10):3174–81.

[146] McGuire JA, Joo J, Pietryga JM, Schaller RD, Klimov VI. New aspects of carrier multiplication in semiconductor nanocrystals. Acc Chem Res 2008;41(12):1810–9.

[147] Sukhovatkin V, Hinds S, Brzozowski L, Sargent EH. Colloidal quantum-dot photodetectors exploiting multiexciton generation. Science 2009;324(5934):1542–4.

[148] Johnson JC, Nozik AJ, Michl J. High triplet yield from singlet fission in a thin film of 1,3-diphenylisobenzofuran. J Am Chem Soc 2010;132(46):16302–3.

[149] Jadhav PJ, Mohanty A, Sussman J, Lee J, Baldo MA. Singlet exciton fission in nanostructured organic solar cells. Nano Lett 2011;11(4):1495–8.

[150] Styers-Barnett DJ, Ellison SP, Mehl BP, Westlake BC, House RL, Park C, et al. Exciton dynamics and biexciton formation in single-walled carbon nano-tubes studied with femtosecond transient absorption spectroscopy. J Phys Chem C 2008;112(12):4507–16.

[151] Pijpers J, Hendry E, Milder M, Fanciulli R, Savolainen J, Herek J, et al. Carrier multiplication and its reduction by photodoping in colloidal inas quantum dots. J Phys Chem C 2008;112(12):4783–4.

[152] Pijpers J, Hendry E, Milder M, Fanciulli R, Savolainen J, Herek J, et al. Carrier multiplication and its reduction by photodoping in colloidal inas quantum dots. J Phys Chem C 2007;111(11):4146–52.

[153] Nootz G, Padilha LA, Levina L, Sukhovatkin V, Webster S, Brzozowski L, et al. Size dependence of carrier dynamics and carrier multiplication in pbs quantum dots. Phys Rev B 2011;83(15):155302.

[154] Emerson R. The quantum yield of photosynthesis. Annu Rev Plant Physiol 1958;9(1):1–24.

[155] Duysens L, Amesz J, Kamp B. Two photochemical systems in photosynthesis. Nature 1961;190:510–1.

[156] Ross RT, Calvin M. Thermodynamics of light emission and free-energy storage in photosynthesis. Biophys J 1967;7(5):595–614.

[157] Kok B, Forbush B, McGloin M. Cooperation of charges in photosynthetic o2 evolution–i. a linear four step mechanism. Photochem Photobiol 1970;11(6):457–75.

[158] Schneider TR. Efficiency of photosynthesis as a solar energy converter. Energy Convers 1973;13(3):77–84.

[159] Walker D, Herold A. Can the chloroplast support photosynthesis unaided. Photosynth Organelles: Struct Funct (special issue of Plant and Cell Physiol) 1977:295–310.

[160] Bassham JA. Increasing crop production through more controlled photo-synthesis. Science (United States) 1977;197:630–8.

[161] Bolton JR. Solar fuels. Science 1978;202(4369):705–11.

[162] Bolton JR, Hall DO. The maximum efficiency of photosynthesis*. Photochem Photobiol 1991;53(4):545–8.

[163] Warden JT, Bolton JR. Light-induced paramagnetism in photosynthetic systems. Acc Chem Res 1974;7(6):189–95.

[164] Ross RT, Hsiao T-L. Limits on the yield of photochemical solar energy conversion. J Appl Phys 1977;48(11):4783–5.

[165] Bolton JR, Hall DO. Photochemical conversion and storage of solar energy. Annu Rev Energy 1979;4(1):353–401.

[166] Engel GS, Calhoun TR, Read EL, Ahn T-K, Mančal T, Cheng Y-C, et al. Evidence for wavelike energy transfer through quantum coherence in photosynthetic systems. Nature 2007;446(7137):782–6.

[167] Kassal I, Yuen-Zhou J, Rahimi-Keshari S. Does coherence enhance transport in photosynthesis? J Phys Chem Lett 2013;4(3):362–7.

[168] Andrews DL, Demidov AA. Resonance energy transfer. Chichester: Wiley; 1999.

[169] Scholes GD. Quantum-coherent electronic energy transfer: did nature think of it first? J Phys Chem Lett 2010;1(1):2–8.

[170] Scholes GD. Biophysics: green quantum computers. Nat Phys 2010;6(6):402–3.

[171] Fenna R, Matthews B. Chlorophyll arrangement in a bacteriochlorophyll protein from chlorobium limicola. Nature 1975;258:573–7.

[172] Fenna R, Matthews B, Olson J, Shaw E. Structure of a bacteriochlorophyll-protein from the green photosynthetic bacterium *chlorobium limicola*: crystallographic evidence for a trimer. J Mol Biol 1974;84(2):231–40.

[173] Li Y-F, Zhou W, Blankenship RE, Allen JP. Crystal structure of the bacterio-chlorophyll *a* protein from *chlorobium tepidum*. J Mol Biol 1997;271(3):456–71.

[174] Camara-Artigas A, Blankenship RE, Allen JP. The structure of the fmo protein from chlorobium tepidum at 2.2 å resolution. Photosynth Res 2003;75(1):49–55.

[175] Cheng Y-C, Fleming GR. Dynamics of light harvesting in photosynthesis. Annu Rev Phys Chem 2009;60:241–62.

[176] Panitchayangkoon G, Hayes D, Fransted KA, Caram JR, Harel E, Wen J, et al. Long-lived quantum coherence in photosynthetic complexes at physiological temperature. Proc Natl Acad Sci 2010;107(29):12766–70.

[177] Mohseni M, Rebentrost P, Lloyd S, Aspuru-Guzik A. Environment-assisted quantum walks in photosynthetic energy transfer. J Chem Phys 2008;129(17):174106.

[178] Rebentrost P, Mohseni M, Kassal I, Lloyd S, Aspuru-Guzik A. Environment-assisted quantum transport. New J Phys 2009;11(3):033003.

[179] Rebentrost P, Mohseni M, Aspuru-Guzik A. Role of quantum coherence and environmental fluctuations in chromophoric energy transport. J Phys Chem B 2009;113(29):9942–7.

[180] Ishizaki A, Fleming GR. On the adequacy of the redfield equation and related approaches to the study of quantum dynamics in electronic energy transfer. J Chem Phys 2009;130:234110.

[181] Ishizaki A, Fleming GR. Theoretical examination of quantum coherence in a photosynthetic system at physiological temperature. Proc Natl Acad Sci 2009;106(41):17255–60.

[182] Zhu J, Kais S, Rebentrost P, Aspuru-Guzik A. Modified scaled hierarchical equation of motion approach for the study of quantum coherence in photosynthetic complexes. J Phys Chem B 2011;115(6):1531–7.

[183] Shi Q, Chen L, Nan G, Xu R-X, Yan Y. Efficient hierarchical Liouville space propagator to quantum dissipative dynamics. J Chem Phys 2009;130:084105.

[184] Kramer T, Kreisbeck C, Rodriguez M, Hein B. Efficiency of the energy transfer in the fmo complex using hierarchical equations on graphics processing units. Bull Am Phys Soc 2011;56:38003.

[185] Berkelbach TC, Markland TE, Reichman DR. Reduced density matrix hybrid approach: application to electronic energy transfer. J Chem Phys 2012;136:084104.

[186] Prior J, Chin AW, Huelga SF, Plenio MB. Efficient simulation of strong system–environment interactions. Phys Rev Lett 2010;105(5):050404.

[187] Huo P, Coker D. Iterative linearized density matrix propagation for modeling coherent excitation energy transfer in photosynthetic light harvesting. J Chem Phys 2010;133:184108.

[188] Moix J, Wu J, Huo P, Coker D, Cao J. Efficient energy transfer in light-harvesting systems, iii: the influence of the eighth bacteriochlorophyll on the dynamics and efficiency in fmo. J Phys Chem Lett 2011;2(24):3045–52.

[189] Skochdopole N, Mazziotti DA. Functional subsystems and quantum redun-dancy in photosynthetic light harvesting. J Phys Chem Lett 2011;2(23):2989–93.

[190] Mazziotti DA. Effect of strong electron correlation on the efficiency of photosynthetic light harvesting. J Chem Phys 2012;137:074117.

[191] Nalbach P, Braun D, Thorwart M. Exciton transfer dynamics and quantum-ness of energy transfer in the Fenna–Matthews–Olson complex. Phys Rev E 2011;84(4):041926.

[192] Shabani A, Mohseni M, Rabitz H, Lloyd S. Efficient estimation of energy transfer efficiency in light-harvesting complexes. Phys Rev E 2012;86(1):011915.

[193] Mohseni M, Shabani A, Lloyd S, Rabitz H. Energy-scales convergence for optimal and robust quantum transport in photosynthetic complexes. J Chem Phys 2014;140(3):035102.

[194] Lloyd S, Mohseni M, Shabani A, Rabitz H. The quantum goldilocks effect: on the convergence of timescales in quantum transport. arXiv preprint arXiv:1111.4982.

[195] Kim J-H, Cao J. Optimal efficiency of self-assembling light-harvesting arrays. J Phys Chem B 2010;114(49):16189–97.

[196] Wu J, Liu F, Shen Y, Cao J, Silbey RJ. Efficient energy transfer in light-harvesting systems, i: optimal temperature, reorganization energy and spatial–temporal correlations. New J Phys 2010;12(10):105012.

[197] Vlaming SM, Silbey RJ. Correlated intermolecular coupling fluctuations in photosynthetic complexes. J Chem Phys 2012;136:055102.

[198] Renaud N, Ratner M, Mujica V. A stochastic surrogate hamiltonian approach of coherent and incoherent exciton transport in the Fenna–Matthews–Olson complex. J Chem Phys 2011;135:075102.

[199] Abramavicius D, Mukamel S. Quantum oscillatory exciton migration in photosynthetic reaction centers. J Chem Phys 2010;133:064510.

[200] Yeh S-H, Zhu J, Kais S. Population and coherence dynamics in light harvesting complex ii (lh2). J Chem Phys 2012;137:084110.

[201] Zhu J, Kais S, Aspuru-Guzik A, Rodriques S, Brock B, Love PJ. Multipartite quantum entanglement evolution in photosynthetic complexes. J Chem Phys 2012;137:074112.

[202] Lloyd S. A quantum of natural selection. Nat Phys 2009;5(3):164–6.

[203] Rebentrost P, Mohseni M, Kassal I, Lloyd S, Aspuru-Guzik A. Environment-assisted quantum transport. New J Phys 2009;11(3):033003.

[204] Hoyer S, Sarovar M, Whaley KB. Limits of quantum speedup in photosyn-thetic light harvesting. New J Phys 2010;12(6):065041.

[205] Adolphs J, Renger T. How proteins trigger excitation energy transfer in the fmo complex of green sulfur bacteria. Biophys J 2006;91(8):2778–97.

[206] Dicke R. Coherence in spontaneous radiation processes. Phys Rev 1954;93(1):99.

[207] Rehler NE, Eberly JH. Superradiance. Phys Rev A 1971;3(5):1735.

[208] Fidder H, Knoester J, Wiersma DA. Optical properties of disordered molecular aggregates: a numerical study. J Chem Phys 1991;95:7880.

[209] Zhao Y, Meier T, Zhang WM, Chernyak V, Mukamel S. Superradiance coherence sizes in single-molecule spectroscopy of lh2 antenna complexes. J Phys Chem B 1999;103(19):3954–62.

[210] Palacios MA, de Weerd FL, Ihalainen JA, van Grondelle R, van Amerongen H. Superradiance and exciton (de) localization in light-harvesting complex ii from green plants? J Phys Chem B 2002;106(22):5782–7.

[211] Jin G, Zhang P, Liu Y-x, Sun C. Superradiance of low-density Frenkel excitons in a crystal slab of three-level atoms: the quantum interference effect. Phys Rev B 2003;68(13):134301.

[212] Strk W. Cooperative energy transfer. Phys Lett A 1977;62(5):315–6.

[213] Scholes GD. Designing light-harvesting antenna systems based on super-radiant molecular aggregates. Chem Phys 2002;275(1):373–86.

[214] Lloyd S, Mohseni M. Symmetry-enhanced supertransfer of delocalized quantum states. New J Phys 2010;12(7):075020.

[215] Abasto D, Mohseni M, Lloyd S, Zanardi P. Exciton diffusion length in complex quantum systems: the effects of disorder and environmental fluctuations on symmetry-enhanced supertransfer. Philos Trans R Soc A: Math Phys Eng Sci 2012;370(1972):3750–70.

[216] Peumans P, Yakimov A, Forrest SR. Small molecular weight organic thin-film photodetectors and solar cells. J Appl Phys 2003;93(7):3693–723.

[217] Lunt RR, Giebink NC, Belak AA, Benziger JB, Forrest SR. Exciton diffusion lengths of organic semiconductor thin films measured by spectrally resolved photoluminescence quenching. J Appl Phys 2009;105(5):053711.

[218] High AA, Novitskaya EE, Butov LV, Hanson M, Gossard AC. Control of exciton fluxes in an excitonic integrated circuit. Science 2008;321(5886):229–31.

[219] Dorfman KE, Voronine DV, Mukamel S, Scully MO. Photosynthetic reaction center as a quantum heat engine. Proc Natl Acad Sci 2013;110(8):2746–51.